affinity than MBP-R(WT), while CRM197(R460H) showed ~1.7-fold higher affinity than CRM197. Further studies of the effect of introduction of other R domain mutations into CRM197 are required.

CRM197 has undergone clinical trials for treatment of ovarian cancers. Because CRM197 is a bacteria-derived exogenous polypeptide, it induces immune responses to eliminate itself. In particular, childhood vaccination against diphtheria, e.g. as a Diphtheria/Pertussis/Tetanus vaccine, has made it easy to enhance anti-DT antibody production. Anti-DT antibodies cross-react with CRM197, and may neutralize the therapeutic activity of CRM197. To avoid such immune responses, it would be necessary to develop CRM197 derivatives with much higher potential to reduce treatment time periods. In this study, we succeeded in generating CRM197(R460H) with a higher affinity to HB-EGF than CRM197 based on the result of R domain mutant protein screening, implicating the inhibitory potential of CRM197 could be further improved by mutagenesis. This study also showed that some R domain mutations did not change the inhibitory activity. R domain mutants themselves or CRM197 with such mutations are expected to show lower reactivity to anti-DT antibodies, and may have a potential use in therapeutics. Combination of appropriate mutations in the R domain may allow us to obtain more potent therapies for cancer and other diseases in which HB-EGF is involved.

Supplementary Data

Supplementary Data are available at *JB* Online.

Acknowledgements

The authors thank Mrs Tomoko Yoneda for technical assistance and Dr Diana Mark Oram (FDA, MA, USA) for providing the pK-PIM vector.

Funding

This work was supported by a Grant-in aid for Scientific Research (A) (23240126 and 26250033 to E.M.) from the Ministry of Education, Culture, Sports, Science and Technology of Japan.

Conflict of Interest

None declared.

References

1. Massague, J. and Pandiella, A. (1993) Membrane-anchored growth factors. *Annu. Rev. Biochem.* **62**, 515–541
2. Prenzel, N., Zwick, E., Daub, H., Leserer, M., Abraham, R., Wallasch, C., and Ullrich, A. (1999) EGF receptor transactivation by G-protein-coupled receptors requires metalloproteinase cleavage of proHB-EGF. *Nature* **402**, 884–888
3. Blobel, C.P. (2005) ADAMs: key components in EGFR signalling and development. *Nat. Rev. Mol. Cell Biol.* **6**, 32–43
4. Higashiyama, S., Abraham, J.A., Miller, J., Fiddes, J.C., and Klagsbrun, M. (1991) A heparin-binding growth factor secreted by macrophage-like cells that is related to EGF. *Science* **251**, 936–939
5. Higashiyama, S., Abraham, J.A., and Klagsbrun, M. (1993) Heparin-binding EGF-like growth factor stimulation of smooth muscle cell migration: dependence on interactions with cell surface heparan sulfate. *J. Cell Biol.* **122**, 933–940
6. Elenius, K., Paul, S., Allison, G., Sun, J., and Klagsbrun, M. (1997) Activation of HER4 by heparin-binding EGF-like growth factor stimulates chemotaxis but not proliferation. *EMBO J.* **16**, 1268–1278
7. Raab, G. and Klagsbrun, M. (1997) Heparin-binding EGF-like growth factor. *Biochim. Biophys. Acta.* **1333**, F179–199
8. Mizushima, H., Wang, X., Miyamoto, S., and Mekada, E. (2009) Integrin signal masks growth-promotion activity of HB-EGF in monolayer cell cultures. *J. Cell Sci.* **122**, 4277–4286
9. Takazaki, R., Shishido, Y., Iwamoto, R., and Mekada, E. (2004) Suppression of the biological activities of the epidermal growth factor (EGF)-like domain by the heparin-binding domain of heparin-binding EGF-like Growth Factor. *J. Biol. Chem.* **279**, 47335–47343
10. Koshikawa, N., Mizushima, H., Minegishi, T., Iwamoto, R., Mekada, E., and Seiki, M. (2010) Membrane type 1-matrix metalloproteinase cleaves off the NH2-terminal portion of heparin-binding epidermal growth factor and converts it into a heparin-independent growth factor. *Cancer Res.* **70**, 6093–6103
11. Iwamoto, R. and Mekada, E. (2006) ErbB and HB-EGF signaling in heart development and function. *Cell Struct. Funct.* **31**, 1–14
12. Iwamoto, R., Yamazaki, S., Asakura, M., Takashima, S., Hasuwa, H., Miyado, K., Adachi, S., Kitakaze, M., Hashimoto, K., Raab, G., Nanba, D., Higashiyama, S., Hori, M., Klagsbrun, M., and Mekada, E. (2003) Heparin-binding EGF-like growth factor and ErbB signaling is essential for heart function. *Proc. Natl. Acad. Sci. USA.* **100**, 3221–3226
13. Minami, S., Iwamoto, R., and Mekada, E. (2008) HB-EGF decelerates cell proliferation synergistically with TGFalpha in perinatal distal lung development. *Dev. Dyn.* **237**, 247–258
14. Mine, N., Iwamoto, R., and Mekada, E. (2005) HB-EGF promotes epithelial cell migration in eyelid development. *Development* **132**, 4317–4326
15. Shirakata, Y., Kimura, R., Nanba, D., Iwamoto, R., Tokumaru, S., Morimoto, C., Yokota, K., Nakamura, M., Sayama, K., Mekada, E., Higashiyama, S., and Hashimoto, K. (2005) Heparin-binding EGF-like growth factor accelerates keratinocyte migration and skin wound healing. *J. Cell Sci.* **118**, 2363–2370
16. Miyamoto, S., Hirata, M., Yamazaki, A., Kageyama, T., Hasuwa, H., Mizushima, H., Tanaka, Y., Yagi, H., Sonoda, K., Kai, M., Kanoh, H., Nakano, H., and Mekada, E. (2004) Heparin-binding EGF-like growth factor is a promising target for ovarian cancer therapy. *Cancer Res.* **64**, 5720–5727
17. Yamazaki, S., Iwamoto, R., Saeki, K., Asakura, M., Takashima, S., Yamazaki, A., Kimura, R., Mizushima, H., Moribe, H., Higashiyama, S., Endoh, M., Kaneda, Y., Takagi, S., Itami, S., Takeda, N., Yamada, G., and Mekada, E. (2003) Mice with defects in HB-EGF ectodomain shedding show severe developmental abnormalities. *J. Cell Biol.* **163**, 469–475
18. Inui, Y., Higashiyama, S., Kawata, S., Tamura, S., Miyagawa, J., Taniguchi, N., and Matsuzawa, Y.

(1994) Expression of heparin-binding epidermal growth factor in human hepatocellular carcinoma. *Gastroenterology* **107**, 1799–1804

19. Ito, Y., Higashiyama, S., Takeda, T., Yamamoto, Y., Wakasa, K.I., and Matsuura, N. (2001) Expression of heparin-binding epidermal growth factor-like growth factor in pancreatic adenocarcinoma. *Int. J. Pancreatol.* **29**, 47–52
20. Ito, Y., Takeda, T., Higashiyama, S., Noguchi, S., and Matsuura, N. (2001) Expression of heparin-binding epidermal growth factor-like growth factor in breast carcinoma. *Breast Cancer Res. Treat.* **67**, 81–85
21. Naef, M., Yokoyama, M., Friess, H., Buchler, M.W., and Korc, M. (1996) Co-expression of heparin-binding EGF-like growth factor and related peptides in human gastric carcinoma. *Int. J. Cancer* **66**, 315–321
22. Tanaka, Y., Miyamoto, S., Suzuki, S.O., Oki, E., Yagi, H., Sonoda, K., Yamazaki, A., Mizushima, H., Maehara, Y., Mekada, E., and Nakano, H. (2005) Clinical significance of heparin-binding epidermal growth factor-like growth factor and a disintegrin and metalloprotease 17 expression in human ovarian cancer. *Clin. Cancer Res.* **11**, 4783–4792
23. Wang, F., Liu, R., Lee, S.W., Sloss, C.M., Couget, J., and Cusack, J.C. (2007) Heparin-binding EGF-like growth factor is an early response gene to chemotherapy and contributes to chemotherapy resistance. *Oncogene* **26**, 2006–2016
24. Sanui, A., Yotsumoto, F., Tsujioka, H., Fukami, T., Horiuchi, S., Shirota, K., Yoshizato, T., Kawarabayashi, T., Kuroki, M., and Miyamoto, S. (2010) HB-EGF inhibition in combination with various anticancer agents enhances its antitumor effects in gastric cancer. *Anticancer Res.* **30**, 3143–3149
25. Yagi, H., Yotsumoto, F., Sonoda, K., Kuroki, M., Mekada, E., and Miyamoto, S. (2009) Synergistic antitumor effect of paclitaxel with CRM197, an inhibitor of HB-EGF, in ovarian cancer. *Int. J. Cancer.* **124**, 1429–1439
26. Naglich, J.G., Rolf, J.M., and Eidels, L. (1992) Expression of functional diphtheria toxin receptors on highly toxin-sensitive mouse cells that specifically bind radioiodinated toxin. *Proc. Natl. Acad. Sci. USA* **89**, 2170–2174
27. Iwamoto, R., Higashiyama, S., Mitamura, T., Taniguchi, N., Klagsbrun, M., and Mekada, E. (1994) Heparin-binding EGF-like growth factor, which acts as the diphtheria toxin receptor, forms a complex with membrane protein DRAP27/CD9, which up-regulates functional receptors and diphtheria toxin sensitivity. *Embo J.* **13**, 2322–2330
28. Collier, R.J. (1975) Diphtheria toxin: mode of action and structure. *Bacteriol. Rev.* **39**, 54–85
29. Oram, D.M., and Holmes, R.K. (2006) Diphtheria toxin in *The Comprehensive Sourcebook of Bacterial Protein Toxins* (Alouf, J.E. and Popoff, M.R., eds.), 245–256, Elsevier, San Diego
30. Choe, S., Bennett, M.J., Fujii, G., Curmi, P.M., Kantardjieff, K.A., Collier, R.J., and Eisenberg, D. (1992) The crystal structure of diphtheria toxin. *Nature* **357**, 216–222
31. Mitamura, T., Higashiyama, S., Taniguchi, N., Klagsbrun, M., and Mekada, E. (1995) Diphtheria toxin binds to the epidermal growth factor (EGF)-like domain of human heparin-binding EGF-like growth factor/diphtheria toxin receptor and inhibits specifically its mitogenic activity. *J. Biol. Chem.* **270**, 1015–1019
32. Mitamura, T., Umata, T., Nakano, F., Shishido, Y., Toyoda, T., Itai, A., Kimura, H., and Mekada, E. (1997) Structure-function analysis of the diphtheria toxin receptor toxin binding site by site-directed mutagenesis. *J. Biol. Chem.* **272**, 27084–27090
33. Shishido, Y., Sharma, K.D., Higashiyama, S., Klagsbrun, M., and Mekada, E. (1995) Heparin-like molecules on the cell surface potentiate binding of diphtheria toxin to the diphtheria toxin receptor/membrane-anchored heparin-binding epidermal growth factor-like growth factor. *J. Biol. Chem.* **270**, 29578–29585
34. Collier, R.J. (2001) Understanding the mode of action of diphtheria toxin: a perspective on progress during the 20th century. *Toxicon.* **39**, 1793–1803
35. Honjo, T., Nishizuka, Y., Hayaishi, O., and Kato, I. (1968) Diphtheria-toxin-dependent adenosine diphosphate ribosylation of aminoacyl transferase II and inhibition of protein synthesis. *J. Biol. Chem.* **243**, 3553–3555
36. Uchida, T., Gill, D.M., and Pappenheimer, A.M. Jr. (1971) Mutation in the structural gene for diphtheria toxin carried by temperate phage. *Nat. New Biol.* **233**, 8–11
37. Uchida, T., Pappenheimer, A.M., Jr., and Greany, R. (1973) Diphtheria toxin and related proteins. I. Isolation and properties of mutant proteins serologically related to diphtheria toxin. *J. Biol. Chem.* **248**, 3838–3844
38. Uchida, T., Pappenheimer, A.M., Jr., and Harper, A.A. (1972) Reconstitution of diphtheria toxin from two non-toxic cross-reacting mutant proteins. *Science* **175**, 901–903
39. Giannini, G., Rappuoli, R., and Ratti, G. (1984) The amino-acid sequenc of two non-toxic mutants of diphtheria toxin:CRM45 and CRM197. *Nucleic Acids Res.* **12**, 4063–4069
40. Kageyama, T., Ohishi, M., Miyamoto, S., Mizushima, H., Iwamoto, R., and Mekada, E. (2007) Diphtheria toxin mutant CRM197 possesses weak EF2-ADP-ribosyl activity that potentiates its anti-tumorigenic activity. *J. Biochem.* **142**, 95–104
41. Kimura, Y., Saito, M., Kimata, Y., and Kohno, K. (2007) Transgenic mice expressing a fully nontoxic diphtheria toxin mutant, not CRM197 mutant, acquire immune tolerance against diphtheria toxin. *J. Biochem.* **142**, 105–112
42. Hamaoka, M., Chinen, I., Murata, T., Takashima, S., Iwamoto, R., and Mekada, E. (2010) Anti-human HB-EGF monoclonal antibodies inhibiting ectodomain shedding of HB-EGF and diphtheria toxin binding. *J. Biochem.* **148**, 55–69
43. Yagi, H., Miyamoto, S., Tanaka, Y., Sonoda, K., Kobayashi, H., Kishikawa, T., Iwamoto, R., Mekada, E., and Nakano, H. (2005) Clinical significance of heparin-binding epidermal growth factor-like growth factor in peritoneal fluid of ovarian cancer. *Br. J. Cancer.* **92**, 1737–1745
44. Yasumoto, K., Yamada, T., Kawashima, A., Wang, W., Li, Q., Donev, I.S., Tacheuchi, S., Mouri, H., Yamashita, K., Ohtsubo, K., and Yano, S. (2011) The EGFR ligands amphiregulin and heparin-binding egf-like growth factor promote peritoneal carcinomatosis in CXCR4-expressing gastric cancer. *Clin. Cancer Res.* **17**, 3619–3630
45. Iwamoto, R., Handa, K., and Mekada, E. (1999) Contact-dependent growth inhibition and apoptosis of epidermal growth factor (EGF) receptor-expressing cells by the membrane-anchored form of heparin-binding

EGF-like growth factor. *J. Biol. Chem.* **274**, 25906–25912

46. Kanei, C., Uchida, T., and Yoneda, M. (1977) Isolation from *Corynebacterium diphtheriae* C7(beta) of bacterial mutants that produce toxin in medium with excess iron. *Infect Immun.* **18**, 203–209
47. Oram, M., Woolston, J.E., Jacobson, A.D., Holmes, R.K., and Oram, D.M. (2007) Bacteriophage-based vectors for site-specific insertion of DNA in the chromosome of Corynebacteria. *Gene* **391**, 53–62
48. Kinjo, A.R., Suzuki, H., Yamashita, R., Ikegawa, Y., Kudou, T., Igarashi, R., Kengaku, Y., Cho, H., Standley, D.M., Nakagawa, A., and Nakamura, H. (2012) Protein Data Bank Japan (PDBj): maintaining a structural data archive and resource description framework format. *Nucleic Acids Res.* **40**, D453–460
49. Kinoshita, K., and Nakamura, H. (2004) eF-site and PDBjViewer: database and viewer for protein functional sites. *Bioinformatics (Oxford, England)* **20**, 1329–1330
50. Louie, G.V., Yang, W., Bowman, M.E., and Choe, S. (1997) Crystal structure of the complex of diphtheria toxin with an extracellular fragment of its receptor. *Mol. Cell* **1**, 67–78
51. Shen, W.H., Choe, S., Eisenberg, D., and Collier, R.J. (1994) Participation of lysine 516 and phenylalanine 530 of diphtheria toxin in receptor recognition. *J. Biol. Chem.* **269**, 29077–29084
52. Lory, S., and Collier, R.J. (1980) Diphtheria toxin: nucleotide binding and toxin heterogeneity. *Proc. Natl. Acad. Sci. USA* **77**, 267–271
53. Seto, Y., Komiya, T., Iwaki, M., Kohda, T., Mukamoto, M., Takahashi, M., and Kozaki, S. (2008) Properties of corynephage attachment site and molecular epidemiology of Corynebacterium ulcerans isolated from humans and animals in Japan. *Jpn. J Infect. Dis.* **61**, 116–122

ANTICANCER RESEARCH *34*: 4615-4620 (2014)

Pre-clinical Study of BK-UM, a Novel Inhibitor of HB-EGF, for Ovarian Cancer Therapy

SUNG OUK NAM[1,2,3,*], FUSANORI YOTSUMOTO[2,3,*], KOHEI MIYATA[1,2,3], YUKI SUZAKI[4], HIROSHI YAGI[5], TAKASHI ODAWARA[6], SADAO MANABE[6], TOYOKAZU ISHIKAWA[6], MASAHIDE KUROKI[2], EISUKE MEKADA[7] and SHINGO MIYAMOTO[1,3]

Departments of [1]Obstetrics and Gynecology, and [2]Biochemistry, Faculty of Medicine, and [3]Central Research Institute for Advanced Molecular Medicine, Fukuoka University, Fukuoka, Japan; [4]Medical Center for Translational Research, Osaka University Hospital, Osaka, Japan; [5]Department of Obstetrics and Gynecology, Graduate School of Medical Sciences, Kyushu University, Fukuoka, Japan; [6]Kanonji Institute, Research Foundation for Microbial Diseases of Osaka University, Kagawa, Japan; [7]Department of Cell Biology, Research Institute for Microbial Diseases, Osaka University, Osaka, Japan

Abstract. *Background/Aim: Heparin-binding epidermal growth factor-like growth factor (HB-EGF), a member of the epidermal growth factor family, is a target for ovarian cancer therapy. The present study investigated the administration schedule of BK-UM, an anticancer agent targeting HB-EGF. Materials and Methods: The ovarian cancer cell line, RMG-I, was injected subcutaneously into five-week-old female nude mice. The BK-UM was administered intraperitoneally, using three administration schedules with different doses. The tumor volume was calculated every week. Statistical significance was assessed using the Mann–Whitney U-test. Results: At doses >0.1 mg/kg, BK-UM displayed significant antitumor effects, although the antitumor effects and body weights of mice did not significantly differ by dose or by three different administration schedules. At a dose <0.1 mg/kg, however, BK-UM had little inhibitory effect on tumor growth. Conclusion: Daily administration of BK-UM, which has a potentially dose-dependent antitumor effect, may be the optimal schedule for clinical application.*

Ovarian cancer is the most common cause of gynecological cancer-related death (1, 2). As ovarian cancer cells are widely spread through the peritoneal cavity by the peritoneal fluid, ovarian cancer is most often diagnosed in advanced stages, leading to a poor prognosis. Accumulating evidence indicates that this peritoneal fluid is a rich source of growth factors, termed ovarian cancer-activating factors (OCAFs), which promote the survival and proliferation for ovarian cancer cells (3). We have previously reported that heparin-binding epidermal growth factor-like growth factor (HB-EGF) is the most widely expressed OCAF, and has a pivotal role in ovarian cancer progression (4, 5). We, therefore, considered HB-EGF to be a therapeutic target for ovarian cancer (6).

HB-EGF is a member of the epidermal growth factor superfamily, and can bind to the epidermal growth factor receptor (EGFR). Membrane-anchored HB-EGF (proHB-EGF) is synthesized similarly to other EGF proteins (7, 8). ProHB-EGF is cleaved by a member of the disintegrin and metalloproteinases family at the cell surface (a mechanism called 'ectodomain shedding'), resulting in soluble HB-EGF (9, 10). As soluble HB-EGF is essential for the formation of some tumors, HB-EGF is a potential therapeutic target for many types of cancer, including ovarian (4, 11), gastric and breast cancer (5, 12, 13).

ProHB-EGF also functions as a diphtheria toxin receptor. Cross-reacting material 197 (CRM197), which has recently been made using a Good Manufacturing Process, designated BK-UM, is a non-toxic mutant of diphtheria toxin (14). BK-UM inhibits the mitogenic action of HB-EGF. BK-UM binds to both the pro- and soluble forms of human HB-EGF, thus inhibiting the binding of HB-EGF to the EGFR (15). However, BK-UM does not inhibit the mitogenic activity of other EGFR ligands, and is therefore recognized as a specific inhibitor of HB-EGF (16). Accordingly, BK-UM is a candidate agent for ovarian cancer treatment, and warrants further investigation. No pre-clinical studies have been

*These Authors contributed equally to this work.

Correspondence to: Dr. Shingo Miyamoto, Department of Obstetrics and Gynecology, Faculty of Medicine, Fukuoka University, 7-45-1 Nanakuma, Jonan-ku, Fukuoka, 814-0180, Japan. Tel: +81 928011011, Fax: +81 928654114, e-mail: smiya@cis.fukuoka-u.ac.jp

Key Words: BK-UM (CRM197), HB-EGF, ovarian cancer, preclinical study.

0250-7005/2014 $2.00+.40

performed to investigate the most effective schedule for BK-UM administration. Therefore, this study aimed to validate the optimal administration of BK-UM in preparation for its investigation in phase I clinical trials in patients with advanced or recurrent ovarian cancer.

Materials and Methods

Reagents. BK-UM, which is composed of CRM197 and is an anticancer agent (15), was obtained from the Research Institute for Microbial Diseases, Osaka University (Osaka, Japan).

Cells and cell culture. A human ovarian cancer cell line, RMG-I, was obtained from the Japanese Collection of Research Bioresources (Osaka, Japan). The cells were maintained in RPMI-1640 medium supplemented with 10% fetal bovine serum (ICN Biomedicals, Irvine, CA, USA), 100 U/ml of penicillin G and 100 μg/ml of streptomycin (Invitrogen Corp., Carlsbad, CA, USA) in a humidified atmosphere of 5% CO_2 at 37°C.

Antitumor effects of BK-UM in a mouse xenograft model. Subconfluent cell cultures were detached from plates with trypsin-EDTA. A total volume of 250 μl containing 5×10^6 cells suspended in serum-free RPMI-1640 was injected subcutaneously into five-week-old female nude mice (Charles River Laboratories Japan Inc., Yokohama, Japan). To assess the inhibitory effects of BK-UM on tumor growth, different doses (5, 10, 25 or 50 mg/kg) of BK-UM were injected intraperitoneally into tumor-bearing mice by three different schedules after the tumor reached an estimated volume of more than 100 mm^3. The BK-UM was administered 10 times during the course of the treatment. The first schedule was daily administration of BK-UM for 10 days. The second schedule was administration of BK-UM on alternate days for 21 days. The third schedule was weekly administration of BK-UM for 10 weeks. Tumor size and body weight of mice were measured every week. The tumor volume was estimated from two-dimensional tumor measurements as follows: tumor volume (mm^3)=(length×width^2)/2.

Statistical analysis. The statistical significance of differences among the groups was assessed using the Mann–Whitney *U*-test. A value of $p<0.05$ was considered statistically significant.

Results

To determine the optimal administration schedule of BK-UM for use in a future clinical study, we examined the antitumor effects on RMG-I xenograft tumor in mice. The tumors treated with 5, 10, 25 or 50 mg/kg of BK-UM using all three administration schedules were significantly smaller by week 11 compared to the initial tumors, and compared to those of control mice ($p<0.05$ for all; Figure 1A-C). However, the tumor sizes and mouse body weights did not significantly differ at week 11 according to doses or schedules of BK-UM administration (Figure 1D-F).

Using the same BK-UM administration schedules, we compared the tumor sizes at week 4 and week 11 for all BK-UM doses. In the daily and alternate-day BK-UM administration groups, the tumor size at week 11 did not significantly differ by dose, whereas the tumor size at week 4 in the group treated with 50 mg/kg of BK-UM tended to be lower compared to mice treated with 5 mg/kg of BK-UM (Figure 2A-D). In the weekly BK-UM administration group, the tumor size at week 4 and week 11 in the 50-mg/kg group showed a small reduction compared to that in the 5 mg/kg groups (Figure 2E and F). Taken together, these results suggest that BK-UM has a dose-dependent antitumor effect.

To assess the overall antitumor effects of BK-UM, we estimated the frequency of the disappearance of tumor at week 11. Daily administration of 5, 10, 25 or 50 mg/kg of BK-UM, and alternate-day administration of 25 or 50 mg/kg of BK-UM made some tumors disappear completely (Figure 3A and B). The frequency of tumor disappearance was highest for mice daily administered 50 mg/kg of BK-UM (Figure 3A). Taken together, these findings suggest that daily BK-UM administration is optimal for inducing antitumor effects.

To confirm that the antitumor effects of BK-UM occur in a dose-dependent manner, we examined the mouse tumor size and body weight after daily administration of 0.01, 0.1, 0.5 or 5 mg/kg of BK-UM. At the 0.1, 0.5 and 5 mg/kg doses of BK-UM, the tumor sizes at week 11 were significantly reduced compared to the control and group treated with 0.01 mg/kg of BK-UM (all $p<0.05$; Figure 4A). However, the body weight of the control mice did not differ significantly in mice treated daily with 0.01, 0.1, 0.5 or 5 mg/kg of BK-UM (Figure 4B).

Discussion

In the present study, BK-UM showed significant, dose-dependent antitumor effects on mice bearing RMG-I xenograft tumors. The daily administration of BK-UM for 10 days yielded the greatest antitumor activity, thus suggesting that daily administration is more effective than the other (alternate day and weekly) schedules.

In ovarian cancer, cytotoxic agents, including carboplatin and paclitaxel, are widely used therapeutic agents. However, most patients with advanced ovarian cancer experience disease relapse within 2 years of initial treatment and ultimately die due to drug resistance. Our previous study has shown that BK-UM effectively suppressed the growth of paclitaxel-resistant cells and had a markedly synergistic antitumor effect when used with paclitaxel (21). In the near future, BK-UM might be used with cisplatin or paclitaxel as a combination therapy for patients with ovarian cancer. In general, chemotherapy for patients with ovarian cancer is performed every three or four weeks as one course. When BK-UM is administered as a single-agent, it should be administered daily. The daily administration of BK-UM could be performed for two weeks, with the subsequent two weeks used as an observation/rest time for one course of chemotherapy.

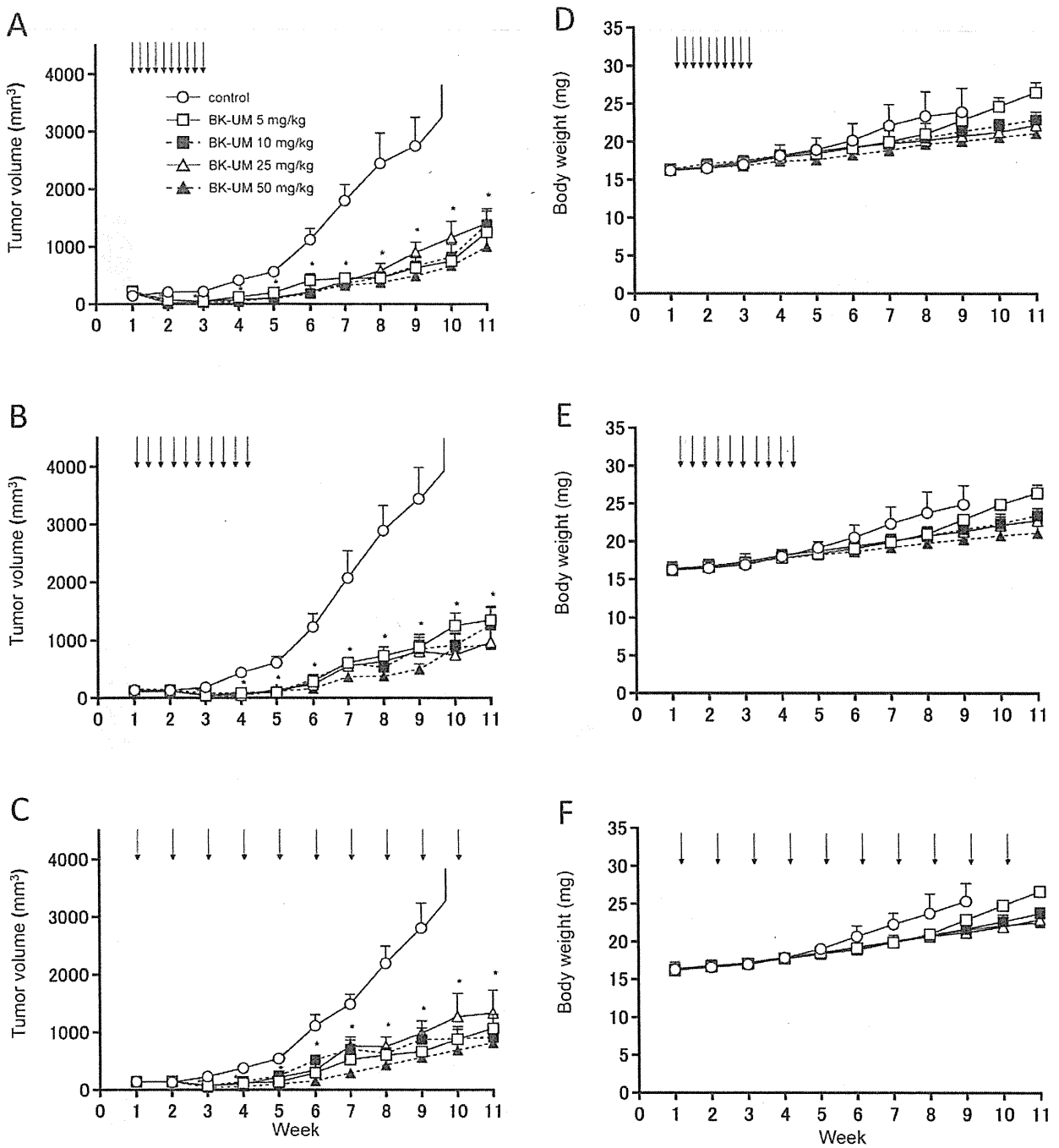

Figure 1. *The effects of BK-UM (CRM197) on the tumor size and body weight of mice bearing RMG-I xenograft tumors. A and D: Daily administration of BK-UM for 10 days. B and E: Administration of BK-UM on alternate days for 21 days. C and F: Weekly administration of BK-UM for 10 weeks. Mice were weighed each time the tumor sizes were measured. Black arrows indicate the days when BK-UM was administered. The number of the mice of all the groups is 6. The tumor volume is presented as the mean±SEM. *p<0.05 versus the control groups for all groups administered BK-UM.*

BK-UM is a mutant form of diphtheria toxin. Although BK-UM is recognized as being non-toxic, its safety has not been reported, and non-mutant diphtheria toxic can induce fatal reactions, such as cardiac arrest. Accordingly, divided BK-UM administration would seem to be safer than using a single injection. Additionally, a previous clinical trial using

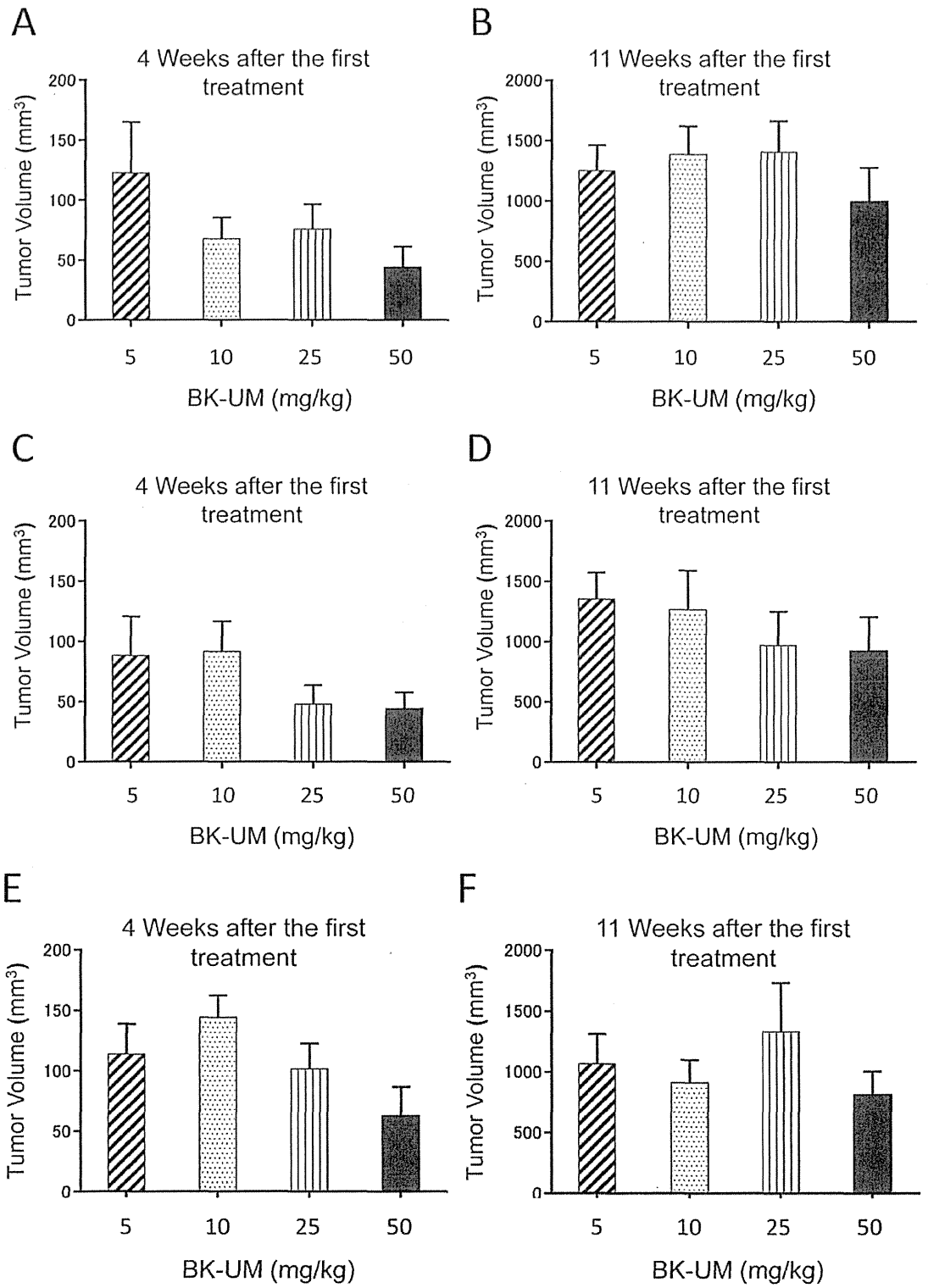

Figure 2. *A comparison of the mean tumor size at the fourth week and eleventh week. The tumor size at week 4 and week 11 after the initial administration of BK-UM was compared for all doses. A and B: Daily administration of BK-UM. C and D: Alternate-day administration of BK-UM. E and F: Weekly administration of BK-UM. The number of the mice of all the groups is 6. Error bars indicate the SEM.*

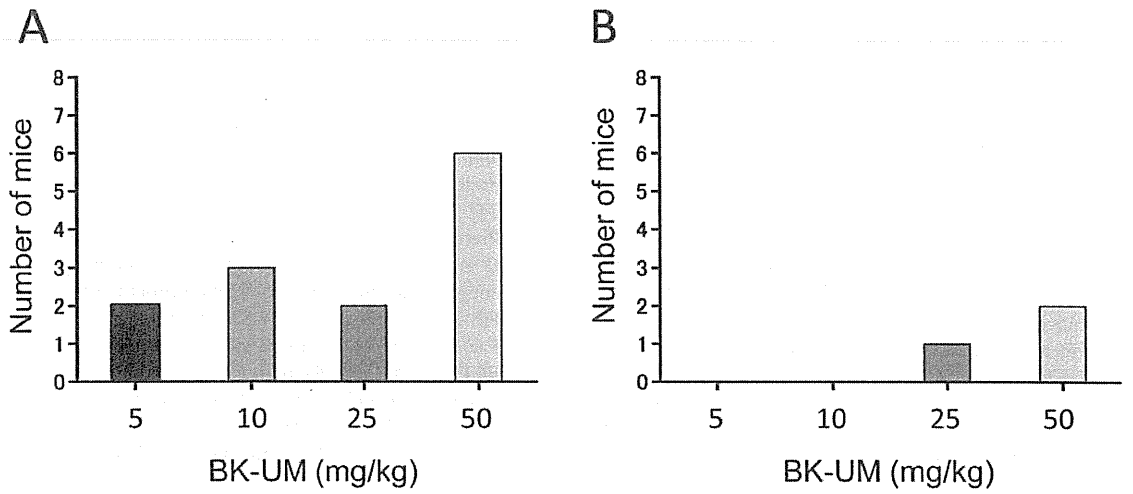

Figure 3. *The frequency of disappearance of the tumor. The number of mice whose tumors disappeared by week 11 after the initial BK-UM administration using daily administration of BK-UM for 10 days (A) and administration of BK-UM on alternate days for 21 days (B). The number of the mice of all the groups is 6.*

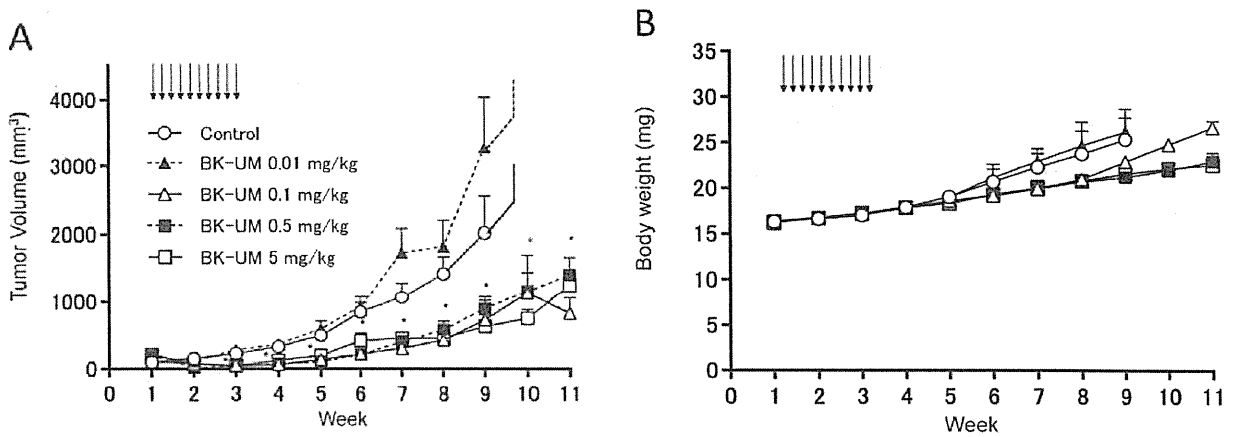

Figure 4. *The dose-dependency of BM-UK when administered daily at the indicated doses for 10 days. A: The tumor volume. B: The mouse body weight. The black arrows indicate the days when BK-UM was administered. The tumor volumes represent the means±SEM. *p<0.05 versus the control or 0.01 mg/kg BK-UM group. The number of the mice of all the groups is 8.*

CRM197 showed that it had a half-life of 16-20 h and a mean half-life of 18.1 h when given subcutaneously (22). Therefore, the daily administration of BK-UM might maintain the serum BK-UM level at a constant, safe and efficacious level.

In conclusion, we have shown that the daily administration of BK-UM was most effective for ovarian cancer therapy in this pre-clinical study, performed as part of Good Laboratory Practice. Pending the approval of our Ethics Committee, a phase I study of BK-UM will be performed at the Fukuoka University for patients with advanced and recurrent ovarian cancer.

References

1 Penson RT, Shannon KE, Sharpless NE and Seiden MV: Ovarian cancer: an update on genetics and therapy. Compr Ther *24*: 477-487, 1998.

2 Friedlander ML: Prognostic factors in ovarian cancer. Semin Oncol *25*: 305-314, 1998.

3 Mills GB, May C, McGill M, Roifman CM and Mellers A: A putative new growth factor in ascetic fluid from ovarian cancer patients: identification, characterization, and mechanism of action. Cancer Res *48*: 1066-1071, 1988.

4 Miyamoto S, Hirata M, Yamazaki A, Kageyama T, Hasuwa H, Mizushima H, Tanaka Y, Yagi H, Sonoda K, Kai M, Kanoh H, Nakano H and Mekada E: Heparin-binding EGF-like growth factor is a promising target for ovarian cancer therapy. Cancer Res *15*: 5720-5727, 2004.
5 Yotsumoto F, Yagi H, Suzuki SO, Oki E, Tsujioka H, Hachisuga T, Sonoda K, Kawarabayashi T, Mekada E and Miyamoto S: Validation of HB-EGF and amphiregulin as targets for human cancer therapy. Biochem Biophys Res Commun *18*: 555-561, 2008.
6 Yagi H, Miyamoto S, Tanaka Y, Sonoda K, Kobayashi H, Kishikawa T, Iwamoto R, Mekada E and Nakano H: Clinical significance of heparin-binding epidermal growth factor-like growth factor in peritoneal fluid of ovarian cancer. Br J Cancer *9*: 1737-1745, 2005.
7 Higashiyama S, Abraham JA, Miller J, Fiddes JC and Klagsbrun MA: Heparin-binding epidermal growth factor secreted by macrophage-like cells that is related to EGF. Science *251*: 936-939, 1991.
8 Massague J and Pandiella A: Membrane-anchored growth factors. Annu Rev Biochem *62*: 515-41, 1993.
9 Miyazono K: Ectodomain shedding of HB-EGF: A potential target for cancer therapy. J. Biochem *151*: 1-3, 2012.
10 Higashiyama S, Nanba D, Nakayama H, Inoue H and Fukuda S: Ectodomain shedding and remnant peptide signalling of EGFRs and their ligands. J. Biochem *150*: 15-22, 2011.
11 Tanaka Y, Miyamoto S, Suzuki SO, Oki E, Yagi H, Sonoda K, Yamazaki A, Mizushima H, Maehara Y, Mekada E and Nakano H: Clinical significance of heparin-binding epidermal growth factor-like growth factor and a disintegrin and metalloprotease 17 expression in human ovarian cancer. Clin Cancer Res *11*: 4783-4792, 2005.
12 Ito Y, Takeda T, Higashiyama S, Noguchi S and Matsuura N: Expression of heparin-binding epidermal growth factor-like growth factor in breast carcinoma. Breast Cancer ResTreat *67*: 81-85, 2001.
13 Murayama Y, Miyagawa J, Shinomura Y, Kanayama S, Isozaki K, Yamamori K, Mizuno H, Ishiguro S, Kiyohara T, Miyazaki Y, Taniguchi N, Higashiyama S and Matsuzawa Y: Significance of the association between heparin-binding epidermal growth factor-like growth factor and CD9 in human gastric cancer. Int J Cancer *98*: 505-513, 2002.
14 Mitamura T, Higashiyama S, Taniguchi N, Klgasbrun M and Mekada E: Diphtheria toxin binds to the epidermal growth factor (EGF)-like domain of human heparin-binding EGF-like growth factor/diphtheria toxin receptor and inhibits specifically its mitogenic activity. J Biol Chem *270*: 1015-1019, 1995.
15 Uchida T, Pappenheimer AM Jr. and Greany R: Diphtheria toxin and related proteins. I. Isolation and properties of mutant proteins serologically related to diphtheria toxin. J Biol Chem *248*: 3838-3844, 1973.
16 Prenzel N, Zwick E, Daub H, Leserer M, Abraham R, Wallasch C and Ullrich A: EGF receptor transactivation by G-protein coupled receptors requires metalloproteinase cleavage of pro-HB-EGF. Nature 402: 884-888, 1999.
17 Faull RJ, Stanley JM, Fraser S, Power DA and Leavesley DI: HB-EGF is produced in the peritoneal cavity and enhances mesothelial cell adhesion and migration. Kidney Int *59*: 614-624, 2001.
18 Jayne DG, Perry SL, Morrison E, Farmery SM and Guillou PJ: Activated mesothelial cells produce heparin-binding growth factors: implications for tumour metastases. Br J Cancer 82: 1233-1238, 2000.
19 Kurman RJ and Shih IM: Molecular pathogenesis and extraovarian origin of epithelial ovarian cancer–Shifting the paradigm. Hum Pathol *42*: 918-931, 2011.
20 Yagi H, Yotsumoto F and Miyamoto S: Heparin-binding epidermal growth factor-like growth factor promotes transcoelomic metastasis in ovarian cancer through epithelial-mesenchymal transition. Mol Cancer Ther *7*: 3441-3451, 2008
21 Yagi H, Yotsumoto F, Sonoda K, Kuroki M, Mekada E and Miyamoto S: Synergistic anti-tumor effect of paclitaxel with CRM197, an inhibitor of HB-EGF, in ovarian cancer. Int J Cancer *15*: 1429-1439, 2009.
22 Buzzi S, Rubboli D, Buzzi G, Buzzi AM, Morisi C and Pironi F: CRM197 (nontoxic diphtheria toxin): effects on advanced cancer patients. Cancer Immunol Immunother *53*: 1041-1048, 2004.

Received April 4, 2014
Revised June 10, 2014
Accepted June 11, 2014

Biochemical and Biophysical Research Communications 449 (2014) 460–465

Contents lists available at ScienceDirect

Biochemical and Biophysical Research Communications

journal homepage: www.elsevier.com/locate/ybbrc

Antibody-modified lipid nanoparticles for selective delivery of siRNA to tumors expressing membrane-anchored form of HB-EGF

Ayaka Okamoto [a], Tomohiro Asai [a], Hiroki Kato [a], Hidenori Ando [a], Tetsuo Minamino [b], Eisuke Mekada [c], Naoto Oku [a,*]

[a] Department of Medical Biochemistry, University of Shizuoka School of Pharmaceutical Sciences, 52-1 Yada, Suruga-ku, Shizuoka 422-8526, Japan
[b] Department of Cardiovascular Medicine, Graduate School of Medicine, Osaka University, 2-2 Yamadaoka, Suita, Osaka 565-0871, Japan
[c] Department of Cell Biology, Research Institute for Microbial Diseases, Osaka University, 2-2 Yamadaoka, Suita, Osaka 565-0871, Japan

ARTICLE INFO

Article history:
Received 2 May 2014
Available online 20 May 2014

Keywords:
siRNA delivery
Lipid nanoparticles
Antibody
HB-EGF
Breast cancer

ABSTRACT

An Fab' antibody against heparin-binding epidermal growth factor-like growth factor (HB-EGF) was applied to achieve advanced tumor-targeted delivery of siRNA. Lipid nanoparticles (LNP) encapsulating siRNA (LNP-siRNA) were prepared, pegylated, and surface modified with Fab' fragments of anti-HB-EGF antibody (αHB-EGF LNP-siRNA). αHB-EGF LNP-siRNA showed high-binding affinity to recombinant human HB-EGF in a Biacore assay. In addition, αHB-EGF LNP-siRNA selectively associated with cells expressing HB-EGF *in vitro*. Confocal microscopic images showed that siRNA formulated in αHB-EGF LNP-siRNA was efficiently internalized into MDA-MB-231 human breast cancer cells, on which HB-EGF is highly expressed. In addition, siRNA encapsulated in αHB-EGF LNP induced obvious suppression of both target mRNA and protein levels in MDA-MB-231 cells. These results indicate that αHB-EGF LNP have excellent potential to deliver siRNA to target cancer cells, resulting in effective gene silencing.

1. Introduction

For clinical application of small interfering RNA (siRNA), many studies have been carried out in both basic and clinical fields [1–3]. Since siRNA is unstable in serum and hardly penetrates the cell membrane, an appropriate siRNA delivery system is necessary for the establishment of siRNA therapies. For this purpose, nanoparticle-mediated delivery of siRNA has been studied to obtain efficient gene silencing [4–6]. Previously, we developed a non-viral vector, named dicetyl phosphate tetraethylenepentamine (DCP-TEPA)-based polycation liposomes (TEPA-PCL), for delivery of double-stranded small RNAs [7]. Our data showed that siRNA or microRNA complexed with TEPA-PCL was highly taken up into cells and had remarkable gene silencing effects [8–10]. Surface modification of TEPA-PCL-based lipoplexes with polyethyleneglycol and peptide ligands, such as Arg-Gly-Asp (RGD)-peptide for targeting integrin $\alpha_v\beta_3$ or Ala-Pro-Arg-Pro-Gly (APRPG)-peptide for targeting vascular endothelial growth factor receptor 1 (VEGFR1), enabled targeted delivery of siRNA and subsequent gene silencing after systemic administration [7,10–12]. On the other hand, we previously designed another type of lipid-based vector for small RNA delivery [13]. We prepared cationic cores carrying siRNA by using palmitoyl RRRRRRGGRRRRG and wrapped them with lipids. lipid nanoparticles (LNP) encapsulating siRNA (LNP-siRNA) thus obtained showed significant gene silencing when they were modified with cell-penetrating peptides on their surface [13].

In the present study, we modified LNP with specific antibody against heparin-binding epidermal growth factor-like growth factor (HB-EGF) to induce gene silencing in target cancer cells in a selective manner. Active targeting of nanoparticles to tumors by antibody conjugation is a promising approach, since tumor cells often express characteristic molecules on their surface that are not found on normal cells [14,15]. HB-EGF is known to be highly expressed on the cell surface of various cancers, such as breast, ovarian, and liver cancers [16,17]. The precursor of HB-EGF is expressed on the cell surface as a membrane-anchored form (proHB-EGF) and then processed to a soluble form (HB-EGF), which mediates the intracellular signaling. Thus, we expected HB-EGF to be a useful target molecule for delivering siRNA to tumors. In fact, our previous study showed that anti-HB-EGF antibody-modified liposomes can efficiently deliver an anticancer agent to cancer cells

Abbreviations: LNP, lipid nanoparticles; LNP-siRNA, LNP encapsulating siRNA; αHB-EGF-LNP, anti-HB-EGF antibody-modified LNP.

* Corresponding author. Fax: +81 54 264 5705.
E-mail address: oku@u-shizuoka-ken.ac.jp (N. Oku).

http://dx.doi.org/10.1016/j.bbrc.2014.05.043
0006-291X/

overexpressing HB-EGF both *in vitro* and *in vivo* [18]. Here, we developed LNP-siRNA modified with Fab' fragments of anti-HB-EGF antibody (αHB-EGF LNP-siRNA) and evaluated their potential as a siRNA vector *in vitro*.

2. Materials and methods

2.1. Materials

siRNA was purchased from Hokkaido System Science Co. (Hokkaido, Japan). In this study, siRNA for the luciferase2 gene was used unless otherwise stated. The nucleotide sequences for enhanced luciferase 2 (siLuc2) were 5′-GCUAUGGGCUGAAUACAA-ATT-3′ (sense) and 5′-UUUGUAUUCAGCCCAUAGCTT-3′ (antisense); and for Lamin A/C (siLamin) with a 2-nucleotide overhang (underline) as 5′-GGUGGUGACGAUCUGGGCUTT-3′ (sense) and 5′-AGCCCAGAUCGUCACCACCTT-3′ (antisense). For the use of fluorescein isothiocyanate (FITC)-labeled siRNA, FITC was conjugated to siLuc2 at the 3′ end of the antisense strand.

A palmitoyl derivative of RRRRRRGGRRRRG peptide was purchased from Operon Biotechnologies (Tokyo, Japan). Dioleoylphosphatidylethanolamine (DOPE), dimyristoylphosphoglycerol (DMPG), distearoylphosphatidylethanolamine (DSPE)-polyethyleneglycol (PEG) 5000 (DSPE-PEG), and maleimide-conjugated DSPE-PEG5000 (DSPE-PEG-maleimide) were purchased from NOF Co. (Tokyo, Japan). Cholesterol was kindly provided by Nippon Fine Chemical Co. (Hyogo, Japan). Monoclonal antibody clone 3E9 specific for HB-EGF was obtained by the method described previously [19]. The 3E9 clone recognizes the EGF-like domain of human proHB-EGF, but not that of mouse proHB-EGF. Recombinant human HB-EGF (rhHB-EGF) was purchased from Wako Pure Chemical Industries, Ltd. (Osaka, Japan).

2.2. Preparation of anti-HB-EGF-modified LNP-siRNA

LNP-siRNA were prepared as described previously [13]. siRNA and palmitoyl RRRRRRGGRRRRG (1/16.8 as a molar ratio, containing 1 nmol of siRNA) dissolved in RNase-free water (1 mL, Invitrogen, Rockville, MD) were mixed and incubated for 30 min at room temperature to obtain the cationic cores. On the other hand, DOPE, cholesterol, and DMPG (6/5/2 as a molar ratio, total lipids: 5 μmol) dissolved in chloroform were evaporated under reduced pressure, and stored *in vacuo* for at least 1 h. LNP-siRNA were prepared by hydration of the thin lipid film with 1 mL of the cationic core solution and sized by use of mild sonication for 3 min at room temperature.

Fab' fragments of anti-HB-EGF monoclonal antibody were prepared as described previously [18]. For the modification of LNP-siRNA with Fab' fragments of anti-HB-EGF antibody, 1 mL of the LNP-siRNA solution was incubated with 45 μL of 5 mM DSPE-PEG and 5 μL of 5 mM DSPE-PEG-maleimide dissolved in RNase free water at 37 °C for 2 h, forming PEG/PEG-maleimide-inserted LNP-siRNA (PEG-mal-LNP-siRNA). The coupling reaction of Fab' fragments with the maleimide moiety of PEG-mal-LNP-siRNA was performed according to the method described earlier [20]. Fab' fragments and PEG-mal-LNP-siRNA (1/1 as a molar ratio of Fab' and maleimide moiety) were mixed, and the coupling reaction was carried out at 4 °C for 16 h. Excess Fab' fragments were separated from the Fab'-coupled PEG-mal-LNP-siRNA by gel-filtration chromatography (Sepharose™ 4 Fast Flow column, GE healthcare, Piscataway, NJ), and the LNP-siRNA fractions were collected. After ultracentrifugation (453,000×*g*, 4 °C, 15 min), anti-HB-EGF Fab'-modified LNP (αHB-EGF LNP-siRNA) were resuspended with 1 mL of RNase- free water. Similarly, the surface of LNP-siRNA was decorated with Fab' fragments of control mouse IgG (MGG-0500, MBL, Nagoya, Japan; Control LNP-siRNA). The particle size and ζ-potential of the particles were measured by using a Zetasizer Nano ZS (Malvern, Worcs, UK).

2.3. Transmission electron microscopy (TEM)

Ten microliters of 5 mM αHB-EGF LNP-siRNA was added onto a grid (Nisshin EM, Tokyo, Japan) and dried-out by warm air. After that, the sample was negatively stained with 10 μL of 1 w/v% ammonium molybdate for 1 min, and imaged with an HT7700 TEM System (Hitachi High-Technologies, Tokyo, Japan). TEM images were recorded with a CCD camera at 1024 × 1024 pixels (Advanced Microscopy Techniques, Woburn, MA).

2.4. Assay to detect binding of αHB-EGF LNP to rhHB-EGF

A Biacore sensor chip was activated with 1-ethyl-3-(3-dimethylaminopropyl)carbodiimide/HCl (EDC) and *N*-hydroxysuccinimide (NHS), and then it was coated with rhHB-EGF dissolved in acetate buffer (pH 4.5). Ethanolamine was used as a blank. PEG-mal-LNP-siRNA, Control LNP-siRNA, or αHB-EGF LNP-siRNA were applied to the sensor chip for binding analysis using the Biacore 2000 system (GE healthcare, Tokyo, Japan) (injection time: 10 min, flow rate: 15 μL/min).

2.5. Cell culture

African green monkey kidney-derived Vero cells overexpressing HB-EGF (Vero-H) [21] were cultured in MEM medium (GIBCO, Grand Island, NY) supplemented with 10% fetal bovine serum (FBS, AusGeneX, Oxenford, Australia), 100 units/mL penicillin G (MP Biomedicals, Irvine, CA), 100 μg/mL streptomycin (MP Biomedicals), and 1 μg/mL G418 (SIGMA-Aldrich, St. Louis, MO) in a CO_2 incubator. MDA-MB-231 human breast cancer cells were cultured in RPMI-1640 medium (Life Technologies, Carlsbad, CA) supplemented with 10% FBS, 100 units/mL penicillin G, and 100 μg/mL streptomycin in a CO_2 incubator.

2.6. siRNA Transfection

Cells were seeded onto a culture plate and pre-cultured overnight. Before transfection, the medium was changed to a fresh one containing FBS but not antibiotics. Control LNP-siRNA or αHB-EGF LNP-siRNA was added to the culture medium at a final concentration of 60 nM (as siRNA), and the cells were then incubated for 24 h at 37 °C in a 5% CO_2 incubator. After a medium change, the cells were incubated for the desired time as described for each experimental procedure.

2.7. Association of αHB-EGF LNP-siRNA with cells overexpressing HB-EGF

Vero-H cells (2×10^4 cells/0.5 mL/well) or MDA-MB-231 cells (4×10^4 cells/0.5 mL/well) were seeded onto 24-well plates (BD Bioscience, San Jose, CA). These cells were incubated for 6, 12 or 24 h with FITC-labeled siRNA (60 nM, Hokkaido System Science Co.) formulated in Control LNP or αHB-EGF LNP. Naked FITC-siRNA was also incubated with the cells as a control. The cells were washed 3 times with PBS and lysed with 1 w/v% n-octyl-β-D-glucoside (Dojindo, Kumamoto, Japan) containing protease inhibitors: 1 mM phenylmethylsulfonyl fluoride (PMSF, Sigma–Aldrich), 2 μg/mL leupeptin (Sigma–Aldrich), 2 μg/mL aprotinin (Sigma–Aldrich), and 2 μg/mL pepstatin A (Sigma–Aldrich). The fluorescence intensity of FITC was determined with a Tecan Infinite M200 microplate reader (Salzburg, Austria) according to the manufacturer's instructions (ex. 485 nm, em. 535 nm) and corrected by total protein content measured with a BCA Protein Assay Reagent

Table 1
Particle size and ζ-potential of nanoparticles.

	Particle size (nm)	PDI	ζ-Potential (mV)
Cationic cores	98.9 ± 2.76	0.29 ± 0.05	+22.0 ± 2.95
LNP-siRNA	134 ± 21.5	0.27 ± 0.03	−40.5 ± 5.30
αHB-EGF LNP-siRNA	161 ± 24.4	0.27 ± 0.07	−9.50 ± 3.78

Size and ζ-potential of nanoparticles were measured by using the Zetasizer Nano ZS. Data are presented as the mean with SD (PDI, polydispersity index).

Kit (PIERCE Biotechnology, Rockford, IL) according to the manufacturer's instructions.

2.8. Cellular uptake of αHB-EGF LNP into MDA-MB-231 cells

MDA-MB-231 cells were seeded onto 8-well chamber slides (Thermo Fisher Scientific, Roskilde, Denmark) at a density of 1×10^4 cells/well and incubated with FITC-labeled siRNA alone (naked siRNA), Control LNP-siRNA or αHB-EGF LNP-siRNA (60 nM as siRNA) for 24 h. After having been washed with PBS, the cells were fixed with 4% paraformaldehyde for 30 min; and the nuclei were then stained with 4′,6-diamidino-2-phenylindole (DAPI, Life Technologies, Carlsbad, CA, USA). Intracellular localization of siRNA was observed by using confocal laser-scanning microscopy (LSM510 META, Carl Zeiss, Germany).

2.9. Gene silencing effect of siRNA formulated in αHB-EGF LNP

The gene silencing effect of αHB-EGF LNP-siRNA was evaluated by use of siLamin. MDA-MB-231 cells were seeded onto 60-mm dishes at a density of 3×10^5 cells/5 mL/dish and then incubated with Control LNP-siLamin or αHB-EGF LNP-siLamin (60 nM as siRNA) for 24 h. The cells were also treated with RNase-free water as a control. Total RNA of the cells was extracted with an RNeasy Plus Mini Kit (QIAGEN, Hilden, Germany) according to the manufacturer's instruction. Then, cDNA was generated from the total RNA samples (5 μg) by use of a Ready-To-Go T-Primed First-Strand Kit (GE Healthcare). In the presence of either human Lamin A/C primers (Takara Bio, Shiga, Japan) or β-actin ones (Takara Bio) and SYBR Premix Ex Taq (Takara Bio), real-time RT-PCR was performed with a Thermal Cycler Dice Real Time System (Takara Bio). The nucleotide sequences of the primers of Lamin A/C were 5′-GAT GAG GAG GGC AAG TTT GTC-3′ (forward) and 5′-AGG GTG AAC TTT GGT GGG AAC-3′ (reverse); and those of β-Actin, 5′-CAT CCG TAA AGA CCT CTA TGC CAA C-3′ (forward) and 5′-ATG GAG CCA CCG ATC CAC A-3′ (reverse). The conditions for real-time RT-PCR were as follow: 95 °C for 30 s, followed by 40 cycles of 95 °C for 5 s, 60 °C for 30 s, 95 °C for 15 s, 60 °C for 30 s, and 95 °C for 15 s.

2.10. Protein-knockdown effect of αHB-EGF LNP-siRNA

Anti-Lamin rabbit polyclonal antibody (Merck Millipore, Billerica, MA), anti-β-actin rabbit polyclonal antibody (Sigma–Aldrich), and horseradish peroxidase (HRP)-conjugated anti-rabbit immunoglobulin G (IgG) polyclonal antibody (GE Healthcare) were used at the dilutions recommended in the manufacturer's instructions.

MDA-MB-231 cells cultured on a 6-well plate (1×10^5 cells/5 mL/dish) were transfected with Control LNP-siLamin or αHB-EGF LNP-siLamin (60 nM as siLamin). After 24 h, the medium

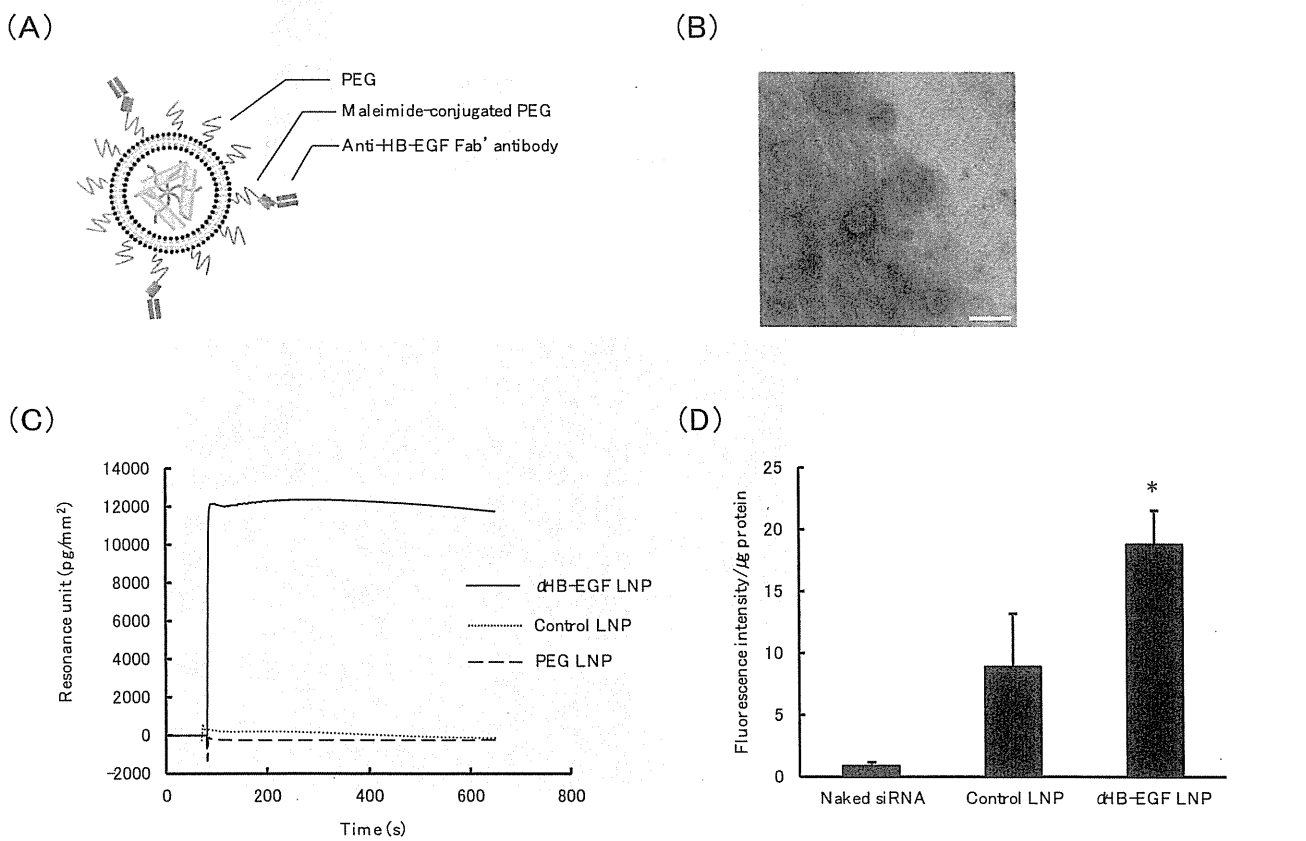

Fig. 1. Characteristics of αHB-EGF LNP-siRNA. (A) Schematic structure of αHB-EGF LNP-siRNA. DSPE-PEG and DSPE-PEG-maleimide were inserted into LNP-siRNA, and the modified nanoparticles were then decorated with anti-HB-EGF Fab' antibody. (B) TEM image of αHB-EGF LNP-siRNA after negative staining with ammonium molybdate. Scale bar indicates 200 nm. (C) Biacore analysis of αHB-EGF LNP-siRNA by use of a sensor chip coated with rhHB-EGF protein. αHB-EGF LNP-siRNA, Control LNP-siRNA or PEG-mal-LNP-siRNA were applied for 10 min to sensitize the sensor chip of the Biacore system. (D) Association of αHB-EGF LNP-siRNA with Vero-H cells. Naked FITC-siRNA (Control) or FITC-siRNA formulated in Control LNP or αHB-EGF LNP was incubated with Vero-H cells for 24 h at 37 °C. After the cells had been lysed, the fluorescence intensity of FITC-siRNA was determined and corrected by the protein contents. An asterisk indicates significant difference ($^*P < 0.05$ *vs.* Control LNP-siRNA).

was changed to a fresh one, and then the cells were cultured for an additional 48 h. The cells were subsequently washed with PBS and lysed with lysis buffer composed of 10 mM Tris–HCl (pH 7.5), 0.15 M NaCl, 0.1% sodium dodecyl sulfate (SDS, Wako Pure Chemical Industries, Ltd.), and protease inhibitors (1 mM PMSF, 2 μg/mL aprotinin, 2 μg/mL leupeptin and 2 μg/mL pepstatin A). Total protein content was measured with a BCA Protein Assay Reagent Kit. Cell lysates were subjected to 10% SDS–PAGE and transferred electrophoretically to a polyvinylidene difluoride (PVDF) membrane (Millipore, Billerica, MA). After having been blocked for 1 h at 37 °C with 5% bovine serum albumin (BSA, Sigma–Aldrich) in Tris–HCl-buffered saline containing 0.1% Tween 20 (TTBS, pH 7.4), the membrane was incubated with a primary antibody against Lamin A/C or β-actin for 24 h at 4 °C, and then with an HRP-conjugated secondary antibody for 1 h at room temperature. Each sample was developed by use of a chemiluminescent substrate (ECL-prime, GE Healthcare), and the chemiluminescence was detected with a LAS-3000 mini system (Fuji Film, Tokyo, Japan).

2.11. Statistical analysis

Differences between groups were evaluated by analysis of variance (ANOVA) with the Tukey *post-hoc* test.

3. Results

3.1. Physicochemical characteristics of αHB-EGF LNP

Particle size and ζ-potential of cationic cores, LNP-siRNA, and αHB-EGF LNP-siRNA are shown in Table 1. Complexes of siRNA and palmitoyl RRRRRRGGRRRRG peptide formed approximately 100-nm cationic cores having a positive charge. LNP-siRNA, i.e., the cores wrapped with lipids containing the anionic phospholipid DMPG, showed an anionic surface charge. The particle size was slightly increased to approximately 130 nm by lipid coating of the cores. After modification of LNP-siRNA with anti-HB-EGF Fab' antibody by using maleimide-PEG-DSPE, the particle size was

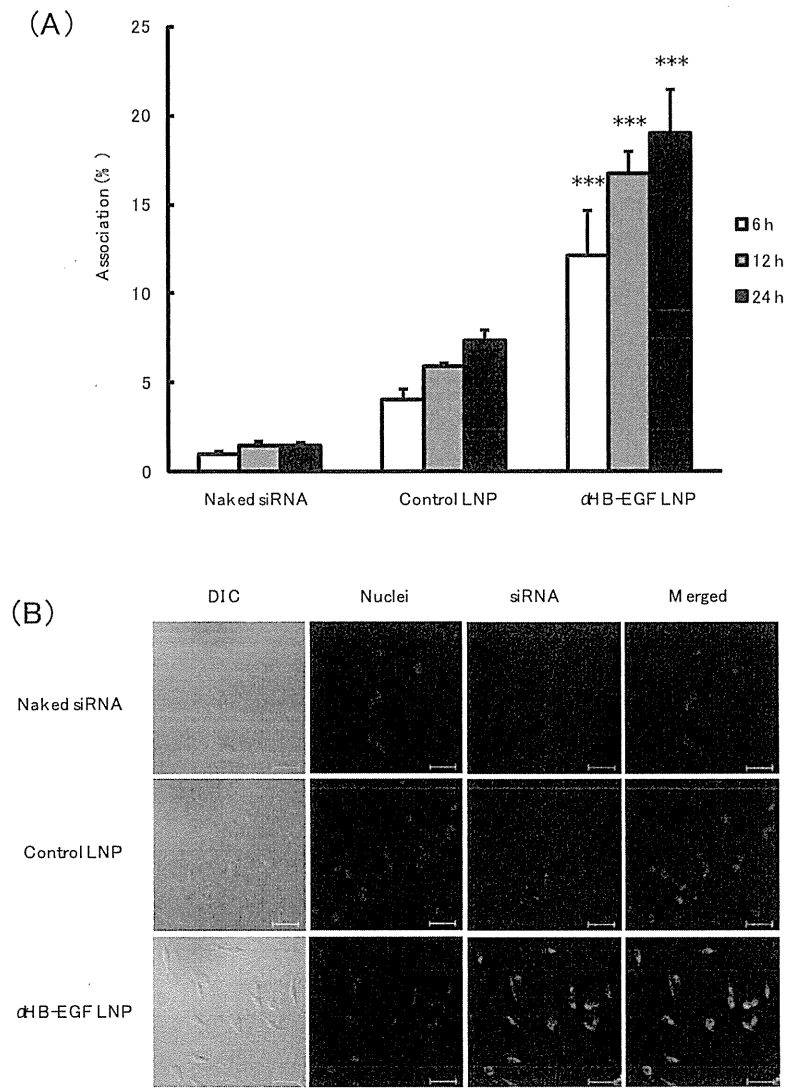

Fig. 2. Uptake of αHB-EGF LNP-siRNA into MDA-MB-231 cells. (A) Association of αHB-EGF LNP-siRNA with MDA-MB-231 cells. Naked FITC-siRNA (Control) or FITC-siRNA formulated in Control LNP or αHB-EGF LNP was incubated with MDA-MB-231 cells for 6, 12 or 24 h at 37 °C. After the cells had been lysed, the fluorescence intensity of the FITC-siRNA was determined. Data are presented as percentages (with SD bars) of siRNA detected in the cell lysate to that in the whole amount added. Asterisks indicate significant differences ($^{***}P < 0.001$ *vs.* Control LNP-siRNA). (B) Intracellular distribution of siRNA in MDA-MB-231 cells that had been transfected with αHB-EGF LNP bearing FITC-labeled siRNA FITC-siRNA (green) taken up into the cells was observed by confocal laser-scanning microscopy. MDA-MB-231 cells were incubated with naked FITC-siRNA, Control LNP-FITC-siRNA, or αHB-EGF LNP-FITC-siRNA for 24 h at 37 °C. The nuclei were stained with DAPI (blue). The scale bars indicate 50 μm. (For interpretation of the references to color in this figure legend, the reader is referred to the web version of this article.)

slightly increased further to approximately 160 nm. The ζ-potential of αHB-EGF LNP-siRNA was closer to neutral compared with that of LNP-siRNA. A schematic structure of αHB-EGF LNP-siRNA is shown in Fig. 1A. Anti-HB-EGF Fab' antibody-grafted DSPE-PEG by using DSPE-PEG-maleimide and non-grafted DSPE-PEG were used to modify the surface of LNP-siRNA. The spherical structure of αHB-EGF LNP-siRNA was confirmed by TEM observation (Fig. 1B). The particle size of αHB-EGF LNP-siRNA observed by TEM was about 150 nm. This result was consistent with the laser light-scattering data. The modification efficiency of the Fab' antibody to PEG-mal-LNP-siRNA was determined using high-performance liquid chromatography. When 25 nmol of the Fab' antibody had been used in the reaction mixture, approximately 15 nmol was recovered in the αHB-EGF LNP-siRNA fraction, indicating a modification efficiency of approx. 60%.

3.2. Targetability of αHB-EGF LNP-siRNA

The binding affinity of αHB-EGF LNP-siRNA for rhHB-EGF protein was assessed by use of a Biacore system having the sensor chip coated with this protein. As a result, αHB-EGF LNP-siRNA showed considerably high binding affinity toward human HB-EGF protein, whereas the Control LNP-siRNA and PEG-LNP-siRNA showed no binding at all (Fig. 1C). Next, FITC-labeled siRNA formulated in αHB-EGF LNP was used to transfect Vero-H cells (Vero cells overexpressing HB-EGF) to determine the targetability of αHB-EGF LNP-siRNA *in vitro*. Twenty-four hours after the transfection, αHB-EGF LNP-siRNA were significantly bound to the surface of the cells and/or taken up into the cells compared to the naked siRNA or Control LNP-siRNA (Fig. 1D).

3.3. Uptake of αHB-EGF LNP-siRNA into MDA-MB-231 cells

Overexpression of HB-EGF in MDA-MB-231 triple-negative breast cancer cells was already demonstrated in our previous study [18]. Here, the association of αHB-EGF LNP-siRNA with MDA-MB-231 cells was examined by use of FITC-labeled siRNA. As shown in Fig. 2A, αHB-EGF LNP-siRNA were significantly bound to the surface of the cells and/or taken up into the cells compared to the naked siRNA or Control LNP-siRNA. In addition, the amount of association increased in a time-dependent manner. Then, the intracellular distribution of FITC-siRNA in the transfected MDA-MB-231 cells was observed by confocal laser-scanning microscopy. As a result, FITC-siRNA delivered in the αHB-EGF LNP was homogeneously distributed throughout the cytoplasm of individual cells (Fig. 2B). In contrast, the fluorescence was quite weak or hardly observed when FITC-siRNA was delivered via the Control LNP-siRNA or applied in its naked form, respectively.

3.4. Gene silencing effects of αHB-EGF LNP-siLamin

After MDA-MB-231 cells had been transfected with αHB-EGF LNP-siLamin, knockdown of Lamin A/C mRNA and protein was determined by use of RT-PCR and Western blotting, respectively. αHB-EGF LNP-siLamin showed approximately 80% knockdown of Lamin A/C mRNA, which was significantly different from that obtained with the control (RNase-free water) or Control LNP-siLamin (Fig. 3A). Control LNP-siLamin showed approximately 50% knockdown of Lamin A/C mRNA. Importantly, the αHB-EGF LNP-siLamin clearly suppressed the expression of Lamin A/C protein compared with the control and Control LNP-siLamin (Fig. 3B).

4. Discussion

Specific antibody is expected to have excellent characteristics for use in targeted delivery of siRNA for the following reasons: the specificity and binding affinity are considerably high [22]; internalization occurs via receptor-mediated endocytosis [23]; and practical utility is demonstrated in the clinical setting [24]. For these reasons, we concluded that LNP modified with an antibody is a promising vector for delivering siRNA into the cytoplasm of target cells safely and specifically.

Therefore, in the present study, we conjugated anti-HB-EGF Fab' antibody to the LNP for targeted delivery of siRNA and showed selective gene silencing using αHB-EGF LNP-siRNA. As was shown in Fig. 1C, αHB-EGF LNP-siRNA significantly bound to rhHB-EGF protein attached to the Biacore chip, indicating that the Fab' fragments of the anti-HB-EGF antibody should function adequately as a targeting ligand. In addition, αHB-EGF LNP-siRNA were significantly associated with Vero-H cells compared to the association obtained with Control LNP-siRNA (Fig. 1D). Such selective association of αHB-EGF LNP-siRNA was not observed with control Vero cells, which hardly express HB-EGF (data not shown). These data suggest that αHB-EGF LNP-siRNA were associated with Vero-H cells via the membrane-anchored form of HB-EGF.

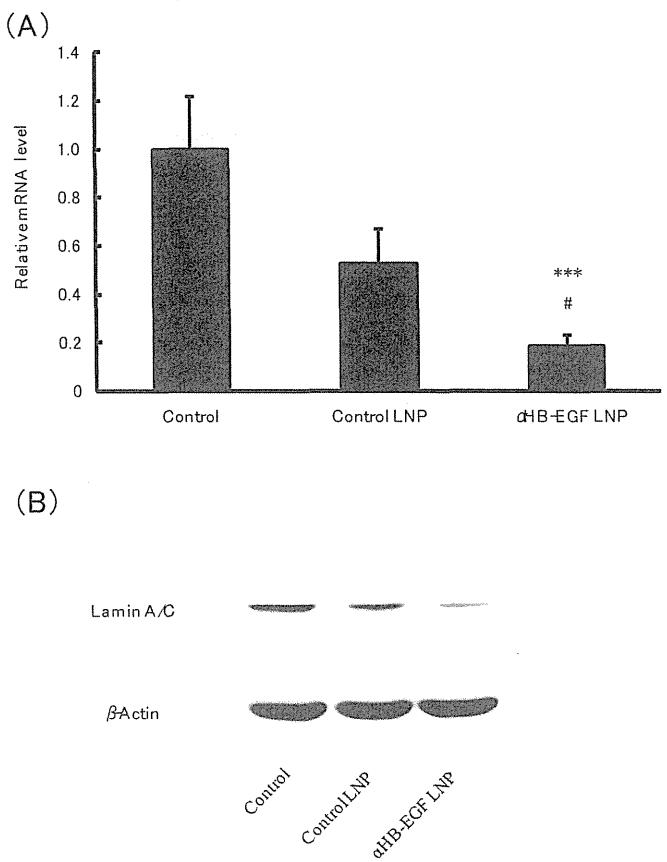

Fig. 3. Gene silencing induced by αHB-EGF LNP-siLamin. (A) Knockdown of Lamin A/C mRNA by αHB-EGF LNP-siLamin. MDA-MB-231 cells were transfected for 24 h with siLamin formulated in Control LNP or αHB-EGF LNP. Other cells were treated with RNase-free water as a control. The expression of Lamin A/C mRNA was determined by real-time RT-PCR. Data are presented as relative expression level of Lamin A/C mRNA to that in the control (RNase-free water) with SD bars. Symbols indicate significant differences ($^{***}P < 0.001$ *vs.* control, $^{\#}P < 0.05$ *vs.* Control LNP). (B) Knockdown of Lamin A/C protein by αHB-EGF LNP-siLamin. MDA-MB-231 cells were incubated for 24 h with siLamin formulated in Control LNP or αHB-EGF LNP. After a medium change, the cells were cultured for an additional 48 h (total of 72 h from the start of transfection). The expression of Lamin A/C and β-actin was determined by Western blotting.

A ligand for the membrane-anchored form of HB-EGF has been reported to be internalized by ligand-mediated receptor endocytosis [25,26]. As expected, αHB-EGF LNP-siRNA were highly taken up into MDA-MB-231 cells which highly express HB-EGF (Fig. 2). Because siRNA was homogeneously distributed throughout the cytoplasm of the cells by delivery in αHB-EGF LNP, the endocytotic pathway via the membrane-anchored form of HB-EGF might be useful for siRNA delivery. The data on gene silencing (Fig. 3) also support efficient and selective siRNA delivery by αHB-EGF LNP.

We previously reported that siRNA encapsulated in LNP is stable even when exposed to 90% FBS for 24 h [13]. In addition, αHB-EGF LNP-siRNA would be expected to have a long half-life in the bloodstream; because the conjugation of Fab' antibody to PEGylated liposomes reportedly does not substantially interfere with their long circulating property [27]. As was shown in Fig. 1B and Table 1, the particle size of αHB-EGF LNP-siRNA appears to be suitable for delivering siRNA to tumors through the gaps in angiogenic vessels. Although *in vivo* studies have not yet been performed, the present findings suggest that αHB-EGF LNP are promising for systemic delivery of siRNA.

Acknowledgment

This research was supported by a Grant-in-Aid for Scientific Research.

References

[1] H.M. Aliabadi, R. Maranchuk, C. Kucharski, P. Mahdipoor, J. Hugh, H. Uludag, Effective response of doxorubicin-sensitive and -resistant breast cancer cells to combinational siRNA therapy, J. Control Release 172 (2013) 219–228.
[2] Y. Wang, Z. Xu, S. Guo, et al., Intravenous delivery of siRNA targeting CD47 effectively inhibits melanoma tumor growth and lung metastasis, Mol. Ther. 21 (2013) 1919–1929.
[3] S.T. Chan, N.C. Yang, C.S. Huang, J.W. Liao, S.L. Yeh, Quercetin enhances the antitumor activity of trichostatin A through upregulation of p53 protein expression in vitro and in vivo, PLoS One 8 (2013) e54255.
[4] Y. Sakurai, H. Hatakeyama, Y. Sato, et al., RNAi-mediated gene knockdown and anti-angiogenic therapy of RCCs using a cyclic RGD-modified liposomal-siRNA system, J. Control Release 173C (2013) 110–118.
[5] P. Liu, H. Yu, Y. Sun, M. Zhu, Y. Duan, A mPEG-PLGA-b-PLL copolymer carrier for adriamycin and siRNA delivery, Biomaterials 33 (2012) 4403–4412.
[6] H. Lee, A.K. Lytton-Jean, Y. Chen, et al., Molecularly self-assembled nucleic acid nanoparticles for targeted in vivo siRNA delivery, Nat. Nanotechnol. 7 (2012) 389–393.
[7] T. Asai, S. Matsushita, E. Kenjo, et al., Dicetyl phosphate-tetraethylenepentamine-based liposomes for systemic siRNA delivery, Bioconjug. Chem. 22 (2011) 429–435.
[8] H. Ando, A. Okamoto, M. Yokota, et al., Development of a miR-92a delivery system for anti-angiogenesis-based cancer therapy, J. Gene Med. 15 (2013) 20–27.
[9] H. Ando, A. Okamoto, M. Yokota, T. Asai, T. Dewa, N. Oku, Polycation liposomes as a vector for potential intracellular delivery of microRNA, J. Gene Med. 15 (2013) 375–383.
[10] H. Koide, T. Asai, K. Furuya, et al., Inhibition of Akt (ser473) phosphorylation and rapamycin-resistant cell growth by knockdown of mammalian target of rapamycin with small interfering RNA in vascular endothelial growth factor receptor-1-targeting vector, Biol. Pharm. Bull. (2011) 602–608.
[11] E. Kenjo, T. Asai, N. Yonenaga, et al., Systemic delivery of small interfering RNA by use of targeted polycation liposomes for cancer therapy, Biol. Pharm. Bull. 36 (2013) 287–291.
[12] N. Yonenaga, E. Kenjo, T. Asai, et al., RGD-based active targeting of novel polycation liposomes bearing siRNA for cancer treatment, J. Control Release 160 (2012) 177–181.
[13] T. Asai, T. Tsuzuku, S. Takahashi, et al., Cell-penetrating peptide-conjugated lipid nanoparticles for siRNA delivery, Biochem. Biophys. Res. Commun. 444 (2014) 599–604.
[14] J.C. Brenner, B. Ateeq, Y. Li, et al., Mechanistic rationale for inhibition of poly(ADP-ribose) polymerase in ETS gene fusion-positive prostate cancer, Cancer Cell 19 (2011) 664–678.
[15] A. Mishra, S. Liu, G.H. Sams, et al., Aberrant overexpression of IL-15 initiates large granular lymphocyte leukemia through chromosomal instability and DNA hypermethylation, Cancer Cell 22 (2012) 645–655.
[16] S. Miyamoto, H. Yagi, F. Yotsumoto, T. Kawarabayashi, E. Mekada, Heparin-binding epidermal growth factor-like growth factor as a novel targeting molecule for cancer therapy, Cancer Sci. 97 (2006) 341–347.
[17] P.P. Ongusaha, J.C. Kwak, A.J. Zwible, et al., HB-EGF is a potent inducer of tumor growth and angiogenesis, Cancer Res. 64 (2004) 5283–5290.
[18] K. Nishikawa, T. Asai, H. Shigematsu, et al., Development of anti-HB-EGF immunoliposomes for the treatment of breast cancer, J. Control Release 160 (2012) 274–280.
[19] M. Hamaoka, I. Chinen, T. Murata, S. Takashima, R. Iwamoto, E. Mekada, Anti-human HB-EGF monoclonal antibodies inhibiting ectodomain shedding of HB-EGF and diphtheria toxin binding, J. Biochem. 148 (2010) 55–69.
[20] T. Ishida, D.L. Iden, T.M. Allen, A combinatorial approach to producing sterically stabilized (Stealth) immunoliposomal drugs, FEBS Lett. 460 (1999) 129–133.
[21] K. Goishi, S. Higashiyama, M. Klagsbrun, et al., Phorbol ester induces the rapid processing of cell surface heparin-binding EGF-like growth factor: conversion from juxtacrine to paracrine growth factor activity, Mol. Biol. Cell 6 (1995) 967–980.
[22] P. Estep, F. Reid, C. Nauman, et al., High throughput solution-based measurement of antibody-antigen affinity and epitope binding, mAbs 5 (2013) 270–278.
[23] S. Bhattacharyya, R. Bhattacharya, S. Curley, M.A. McNiven, P. Mukherjee, Nanoconjugation modulates the trafficking and mechanism of antibody induced receptor endocytosis, Proc. Natl. Acad. Sci. U.S.A. 107 (2010) 14541–14546.
[24] S. Dou, Y.D. Yao, X.Z. Yang, et al., Anti-Her2 single-chain antibody mediated DNMTs–siRNA delivery for targeted breast cancer therapy, J. Control Release 161 (2012) 875–883.
[25] A. Kimura, M. Terao, A. Kato, et al., Upregulation of N-acetylglucosaminyltransferase-V by heparin-binding EGF-like growth factor induces keratinocyte proliferation and epidermal hyperplasia, Exp. Dermatol. 21 (2012) 515–519.
[26] M. Hieda, M. Koizumi, C. Higashi, T. Tachibana, T. Taguchi, S. Higashiyama, The cytoplasmic tail of heparin-binding EGF-like growth factor regulates bidirectional intracellular trafficking between the plasma membrane and ER, FEBS Open Bio 2 (2012) 339–344.
[27] K. Maruyama, N. Takahashi, T. Tagawa, K. Nagaike, M. Iwatsuru, Immunoliposomes bearing polyethyleneglycol-coupled Fab' fragment show prolonged circulation time and high extravasation into targeted solid tumors in vivo, FEBS Lett. 413 (1997) 177–180.

Gastric Cancer (2014) 17:255–262
DOI 10.1007/s10120-013-0279-1

ORIGINAL ARTICLE

Mortalin is a prognostic factor of gastric cancer with normal p53 function

Koji Ando · Eiji Oki · Yan Zhao · Ayae Ikawa-Yoshida · Hiroyuki Kitao · Hiroshi Saeki · Yasue Kimura · Satoshi Ida · Masaru Morita · Tetsuya Kusumoto · Yoshihiko Maehara

Received: 31 January 2013 / Accepted: 11 June 2013 / Published online: 5 July 2013

Abstract
Background Mortalin is a heat-non-inducible member of the heat shock protein 70 family. Mortalin binds to p53 and prevents p53 from entering the nucleus. To understand the significance of mortalin in gastric cancer, we investigated the expression of mortalin and p53.
Methods Expression of mortalin and p53 was examined by immunohistochemical staining of 182 clinical samples of gastric cancer.
Results Mortalin-positive and aberrant p53-positive tumors were found in 75.2 and 49.5 % of cases, respectively. Mortalin-positive tumors were deeper in invasion and had more lymph node and liver metastases compared with mortalin-negative tumors ($P < 0.01$, $P < 0.05$, respectively). Mortalin-positive tumors had worse prognosis compared with mortalin-negative tumors ($P = 0.035$). Moreover, in tumors with normal p53 function, mortalin-positive tumors had worse prognosis compared with mortalin-negative tumors ($P = 0.017$).
Conclusions Mortalin has a great impact on gastric cancer with normal p53. Therefore, mortalin is a target molecule for treatment of gastric cancer, as well as a promising prognostic factor, especially in tumors with normal p53.

K. Ando · E. Oki (✉) · Y. Zhao · A. Ikawa-Yoshida · H. Saeki · Y. Kimura · S. Ida · M. Morita · T. Kusumoto · Y. Maehara
Department of Surgery and Science, Graduate School of Medical Sciences, Kyushu University, 3-1-1 Maidashi, Higashi-ku, Fukuoka, Fukuoka 821-8582, Japan
e-mail: okieiji@surg2.med.kyushu-u.ac.jp

H. Kitao
Department of Molecular Oncology, Graduate School of Medical Sciences, Kyushu University, 3-1-1 Maidashi, Higashi-ku, Fukuoka, Fukuoka 821-8582, Japan

Keywords Mortalin · p53 · Prognostic factor

Introduction

Gastric cancer still has the highest morbidity rate and the second highest mortality rate in Asian countries. Chemotherapy confers only a minimal survival advantage; therefore, the prognosis of patients with advanced or recurrent gastric cancer remains poor. Also, at present, there are few molecular therapies for gastric cancer. Studying the mechanisms and underlying molecules that drive gastric cancer malignancy could contribute to finding a treatment for the disease.

Mortalin was first cloned as a mortality factor in the cytoplasmic fraction of normal, but not in immortal, mouse fibroblasts [1]. Two forms of murine mortalin have been found, mot-1 and mot-2, which differ by two amino acids [2]. Mot-1 is pancytosolic and its overexpression induces cellular senescence, whereas mot-2 is located in the perinuclear region and its overexpression induces malignant transformation. Genetic cloning has not revealed the existence of more than one human mortalin cDNA. Human mortalin has been found to have transforming activity similar to that of murine mot-2 [3]. Mortalin is known to be expressed in various stress responses such as glucose deprivation, low-dose ionising radiation, and caloric restriction [4–6]. Also, mortalin binds to many proteins [7–9], including tumor suppressor p53. Mortalin sequesters p53 in the cytoplasm and inhibits its normal transcriptional activation [10, 11]. Mortalin and p53 form a complex in the cytoplasm or in the centrosome, which also compromises p53 activity, and thus prevents apoptosis under stress conditions. It has also been reported that upregulation of mortalin contributes to human carcinogenesis [12]. By

contrast, downregulation of mortalin results in growth arrest in immortalized human cells [13]. Mortalin seems to be important for cancer cells in carcinogenesis and proliferation. In colorectal cancer, overexpression of mortalin is correlated with poor outcome [14].

However, to date, no studies have shown the relationship between mortalin and p53 expression in human cancer. Here, we report the significance of mortalin in normal p53-expression gastric cancer by analyzing clinical samples.

Materials and methods

Tissue samples

This study included 182 unselected Japanese patients with primary gastric cancer. All of the patients underwent gastrectomy between 1994 and 2006 at the Department of Surgery and Science, Graduate School of Medical Sciences, Kyushu University Hospital, Fukuoka, Japan. One hundred eighteen men and 64 women were included, ranging from 29 to 90 years of age (mean, 63.8 years). Informed consent was obtained from all patients, and those who did not agree to the study were excluded. A thorough histological examination was carried out with hematoxylin-and-eosin-stained tissue preparations, and classification was made according to the general rules established by the Japanese Gastric Cancer Association [15]. No patients who were treated preoperatively with cytotoxic drugs were included in this study.

Immunohistochemical staining of mortalin and p53

Formalin-fixed, paraffin-embedded tissue specimens were used for immunohistochemical staining. A paraffin block contained both cancerous and adjacent non-cancerous tissue, and cancerous tissue that invaded the deepest area of the stomach wall was selected in all cases. Sections 5 μm thick from paraffin-embedded blocks were deparaffinised in xylene and rehydrated in a graded series of ethanol. Procedures for immunohistochemical staining have been described previously [14]. The sections were pretreated with autoclaving at 121 °C for 15 min in 0.01 mol/l citrate-buffered saline (pH 6.0) for antigen retrieval. Endogenous peroxidase activity was blocked by incubation with 3 % H_2O_2 for 30 min at room temperature. The sections were incubated with 10 % normal goat serum for 1 h to block non-specific binding of the immunological reagents. After incubation with mouse monoclonal antibodies against mortalin (Clone JG1, 1:50; Affinity BioReagents, Golden, CO, USA) at 4 °C overnight, streptavidin-biotin complex and horseradish peroxidase were applied, and reaction products were visualized using the Histofine SAB-PO (M) immunohistochemical staining kit (Nichirei, Tokyo, Japan), according to the manufacturer's instructions. The peroxidase labeling was developed by incubation of the sections in diaminobenzidine tetrahydrochloride for 3 min. Finally, nuclear counterstaining was done using Mayer's hematoxylin solution. Two blinded observers (K.A. and Y.Z.) independently examined the immunostained sections. When >70 % of cytoplasmic-stained cancer cells were included in the section, the tumor was considered to be mortalin-positive.

Expression of p53 was investigated using a monoclonal antibody against p53 (Clone DO-7; Dako Cytomation, Glostrup, Denmark) in the consecutive sections that were used for mortalin staining. The specimens were incubated overnight with a 1:100 dilution of primary antibody at 4 °C. When 70 % or more cancer cells showed positive nuclear staining, then aberrant "positive" staining was defined [16, 17]. And for the rest cases, aberrant "negative" was defined.

The *TP53* gene mutation analysis

The *TP53* gene, exon 5 to exon 9 including exon–intron junctions, were amplified by PCR using "p53 primers" (Nippon Gene, Tokyo, Japan) and Ex Taq DNA polymerase with 3′ exonuclease activity (TaKaRa Bio Inc., Tokyo, Japan). The PCR products were purified and used as templates for cycle sequencing reactions with Big Dye Terminator Cycle Sequencing Kit Version 1.0 (Applied Biosystems). Mutations found in a PCR product were verified by reverse sequencing and reconfirmed in two independently amplified PCR products.

Statistical analysis

Statistical analysis was performed by using JMP 6.0 software (SAS institute, Cary, NC, USA). The χ^2 test, Fisher's exact test, and one-way ANOVA were used as appropriate. A P value <0.05 was considered significant. Kaplan-Meier analysis was used for overall survival. For multivariate analysis, Cox regression analysis was performed using the factors that were significant for overall survival.

Results

Expression of p53 in gastric cancer

It is widely recognized that, in tumors with *TP53* gene mutation, overexpression of aberrant p53 can be stained immunohistochemically [18]. Consistent with previous studies, the expression of positive aberrant p53 was seen in

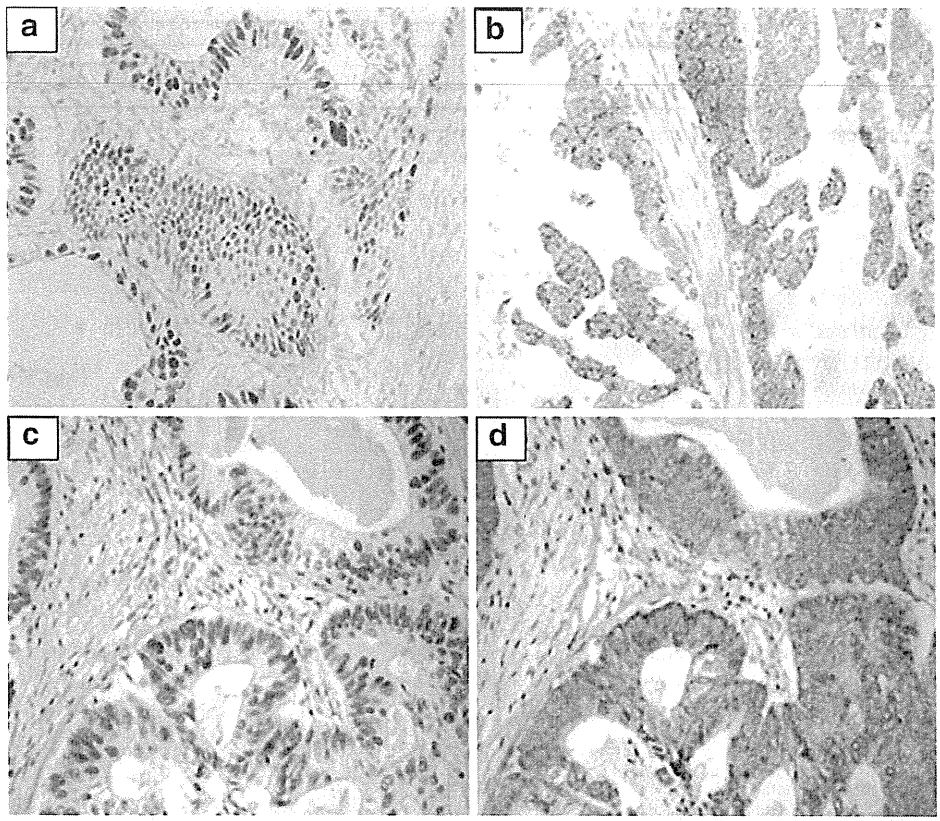

Fig. 1 Expression of aberrant p53 and mortalin in gastric cancer. **a** Staining pattern of tumors with aberrant p53 (magnification, ×400). Aberrant p53 can be seen in the nuclei. **b** Staining pattern of tumors with mortalin expression (magnification, ×400). Mortalin can be seen in the cytoplasm. Staining pattern of aberrant p53 (**c**) and mortalin (**d**) in consecutive sections of the same sample. Mortalin-positive tumor cells expressed aberrant p53

the nuclei of tumor cells (Fig. 1a) [16, 17]. Of 182 tumors, 90 (49.5 %) had positive expression of aberrant p53. With clinicopathological analysis (Table 1), aberrant p53-positive tumors had deeper invasion ($P < 0.05$). In addition, aberrant p53 positive tumors had more lymph node and liver metastases compared with tumors with negative aberrant p53 staining ($P < 0.01$, $P = 0.001$, respectively). Also, more vascular involvement was seen in aberrant p53-positive tumors ($P < 0.01$). Figure 2a shows the overall survival curve in 182 gastric cancer patients in accordance with p53 expression. As previously reported [19], aberrant p53-positive tumors had worse prognosis than those with aberrant p53-negative tumors ($P = 0.043$).

Significance of p53 immunohistochemistry staining in gastric cancer

To validate whether p53 immunohistochemistry staining reflects the function of p53, we then checked the relation between p53 immunohistochemistry staining and *TP53* gene mutation analysis. According to a report on p53 immunohistochemistry staining in colorectal cancer [17], we re-evaluated p53 staining in three groups. When no cancer cells showed positive nuclear staining, then "null" staining was defined (Fig. 3a). When 10–50 % cancer cells showed positive nuclear staining and sporadic staining of p53, then "scattered" staining was defined (Fig. 3b). When 70 % or more cancer cells showed positive nuclear staining, then "aberrant positive" staining was defined (Fig. 3c).

TP53 gene mutation analysis was done in 90 cases of gastric cancer cases; 17 cases (18.8 %) had mutation in *TP53* gene.

Interestingly, all cases of the scattered staining were *TP53* gene wild type (Table 2). Quite a lot of *TP53* gene mutant cases had aberrant p53 staining (11/17).

From these results, "scattered" staining of p53 may reflect normal function of p53.

Mortalin expression is associated with malignant features in gastric cancer

We then confirmed mortalin expression in consecutive sections of gastric cancer samples that were examined for expression of p53. Mortalin was expressed in the cytoplasm (Fig. 1b), and only the tumor cells expressed mortalin.

Of 182 tumors, 137 (75.2 %) were positive for mortalin staining. Table 1 shows the relationship between the clinicopathological features and mortalin expression in gastric cancer patients. Mortalin-positive tumors showed deeper invasion than mortalin-negative tumors ($P < 0.01$).

Table 1 p53 or mortalin expression and clinicopathological factors in gastric cancer patients

Factors	p53 expression		*P* value	Mortalin expression		*P* value
	Negative ($n = 92$)	Positive ($n = 90$)		Negative ($n = 45$)	Positive ($n = 137$) (%)	
Age (mean ± SD)	64.2 ± 12.4	63.4 ± 11.9	0.61	61.9 ± 13.3	64.5 ± 11.7	0.87
Gender						
Male	59 (64.1)	59 (65.6)	0.84	28 (62.2)	90 (65.7)	0.67
Female	33 (35.9)	31 (34.4)		17 (37.8)	47 (34.3)	
Differentiation						
Differentiated	36 (39.1)	44 (49.4)	0.16	18 (40.0)	62 (45.6)	0.51
Undifferentiated	56 (60.9)	45 (50.6)		27 (60.0)	74 (54.4)	
Vascular involvement						
V0	57 (62.0)	59 (52.2)	0.004*	27 (61.4)	75 (54.7)	0.12
V1	26 (28.3)	27 (23.9)		12 (27.3)	32 (23.4)	
V2	8 (8.7)	18 (15.9)		5 (11.3)	21 (15.3)	
V3	1 (1.0)	9 (8.0)		0 (0)	9 (6.6)	
Lymphatic involvement						
Ly0	31 (33.7)	19 (21.4)	0.14	17 (38.6)	33 (24.1)	0.28
Ly1	20 (21.7)	26 (29.1)		8 (18.2)	38 (27.7)	
Ly2	28 (30.4)	24 (27.0)		12 (27.3)	40 (29.2)	
Ly3	13 (14.1)	20 (22.5)		7 (15.9)	26 (19.0)	
Depth of invasion						
M, SM	16 (17.4)	6 (6.7)	0.02**	11 (24.4)	11 (8.0)	0.006*
MP, SS, SE, SI	76 (82.6)	84 (93.3)		34 (75.6)	126 (92.0)	
Lymph node metastasis						
Negative	38 (41.3)	20 (22.2)	0.005*	21 (46.7)	37 (27.0)	0.016**
Positive	54 (58.7)	70 (77.8)		24 (53.3)	100 (73.0)	
Liver metastasis						
Negative	92 (100)	82 (92.1)	0.001*	44 (100)	130 (94.9)	0.046**
Positive	0 (0)	7 (7.9)		0 (0)	7 (5.1)	
Stage						
I + II	46 (50.0)	36 (40.0)	0.17	25 (55.6)	57 (41.6)	0.1
III + IV	46 (50.0)	54 (60.0)		20 (44.4)	80 (58.4)	

M mucosa, *SM* submucosa, *MP* muscularis propria, *SS* subserosa, *SE* penetration of serosa, *SI* invasion of adjacent structures

* $P < 0.01$

** $P < 0.05$

Furthermore, mortalin-positive tumors had more lymph node and liver metastases compared with mortalin-negative tumors ($P < 0.05$). As shown in Fig. 2b, mortalin-positive tumors had worse prognosis compared with mortalin-negative tumors ($P = 0.023$).

Expression of mortalin and aberrant p53 are significantly related

We examined whether there was a correlation between mortalin and aberrant p53 expression. As shown in Table 3, mortalin and aberrant p53 expression had a significant relationship: tumors that were positive for mortalin also expressed aberrant p53 ($P < 0.001$). Surprisingly, in tumors with expression of aberrant p53 and mortalin, the positively stained cells were exactly the same (Fig. 1c, d), but the proteins were not co-localized in the cells. This was true for all the tumors with co-expression of mortalin and aberrant p53.

Expression of mortalin contributes to malignancy and poor prognosis in tumors with scattered p53 staining

To establish the significance of mortalin, we examined its expression in 75 tumors with scattered staining of p53. As previously mentioned scattered staining of p53 may reflect normal p53 function in gastric cancer (Table 2).

In 75 tumors, 27 were mortalin-negative and 48 were mortalin-positive. With clinicopathological analysis (Table 4), mortalin-positive tumors showed deeper invasion ($P < 0.05$) compared with mortalin-negative tumors. Among these, mortalin-positive tumors ($n = 48$) had worse outcome compared with mortalin-negative tumors (Fig. 4; $P = 0.017$). With multivariate analysis (Table 5), mortalin expression appeared to be an independent prognostic factor in gastric cancer with scattered staining of p53 ($P = 0.013$).

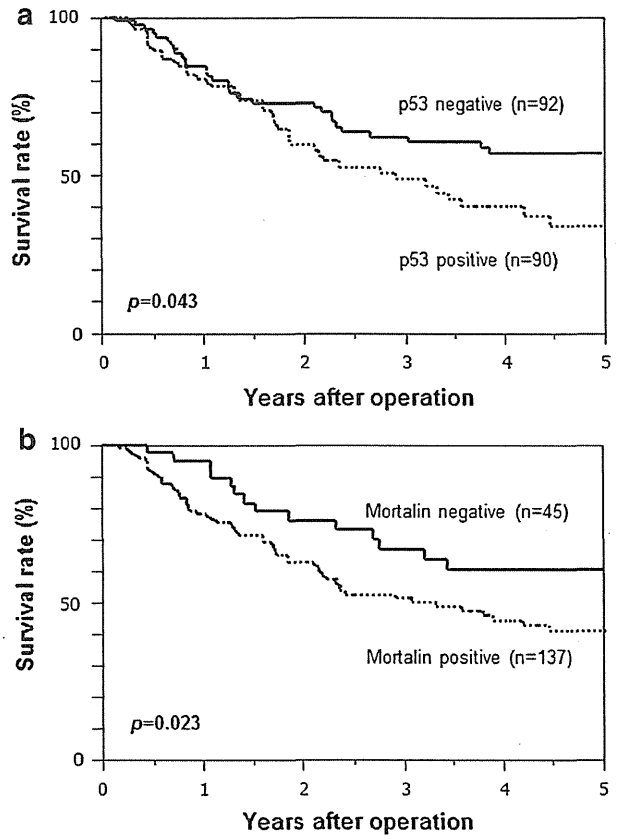

Fig. 2 Cumulative survival curve for gastric cancer patients. **a** Survival curve for gastric cancer patients in accordance with p53 expression. Tumors with expression of aberrant positive p53 had worse prognosis than those with aberrant negative p53 ($n = 182$, $P = 0.043$). **b** Survival curve for gastric cancer patients in accordance with mortalin expression. Mortalin-positive tumors had worse prognosis than mortalin-negative tumors ($n = 182$, $P = 0.023$)

Discussion

In treating gastric cancer, the most commonly used regimens are combination chemotherapy consisting of a fluoropyrimidine (5-fluorouracil or oral fluoropyrimidine) plus a platinum agent with or without docetaxel or anthracyclines. Unlike colorectal cancer, there are few molecular therapies for gastric cancer. In this study, we found that mortalin was highly expressed in gastric cancer and had a high impact on gastric cancer with normal function of p53. Targeting mortalin might be a remedy for gastric cancer in normal p53.

Cancer cells live in a more stressful environment than normal cells do. Because their number is so high, their nutrient and oxygen levels are low. Under stressful conditions, such as DNA damage, UV irradiation, and hypoxia, p53 is phosphorylated or acetylated. The post-translationally modified p53 is an activated form and translates its downstream factors such as *p21*, *BAX*, *PUMA*, and *Noxa* [20–23]. This process causes cell cycle arrest (via p21) or apoptosis. Under normal conditions, p53 is unstable because its half-life is no longer than 20 min owing to cleavage through Mdm2 [24]. Once p53 has been phosphorylated, however, Mdm2 can no longer bind to p53, and activated p53 becomes stable. In cancer, >50 % of tumors have a mutation in the *TP53* gene [25, 26], or Mdm2 is overexpressed [24] by its gene amplification, and normal function of p53 is thus inactivated. We evaluated the expression of Mdm2 in the same sample of gastric cancer used in this study. However, no relation between Mdm2 expression and p53 was observed (data not shown). Although p53 is recognized as an important factor for

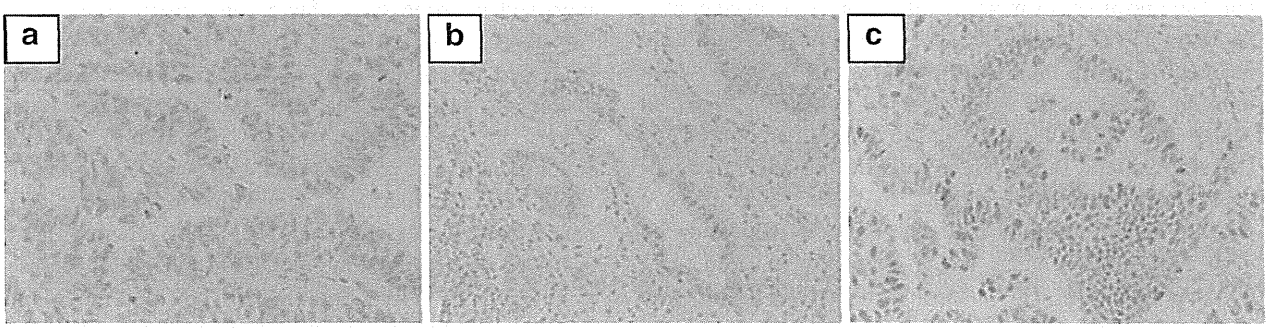

Fig. 3 Classification for p53 staining in gastric cancer. **a** Staining pattern of tumors with "null" staining of p53 (magnification, ×400). **b** Staining pattern of tumors with "scattered" staining of p53 (magnification, ×400). Single cells are stained sporadically. **c** Staining pattern of tumors with "aberrant" staining of p53 (magnification, ×400). All cells are stained widely